

# Negative Ions of Polyatomic Molecules

by L. G. Christophorou\*

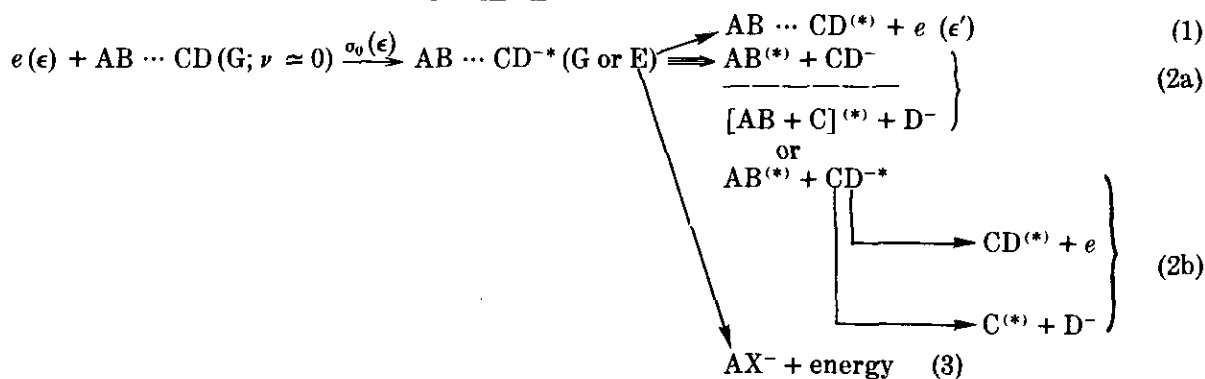
In this paper general concepts relating to, and recent advances in, the study of negative ions of polyatomic molecules are discussed with emphasis on halocarbons. The topics dealt with in the paper are as follows: basic electron attachment processes, modes of electron capture by molecules, short-lived transient negative ions, dissociative electron attachment to ground-state molecules and to "hot" molecules (effects of temperature on electron attachment), parent negative ions, effect of density, nature, and state of the medium on electron attachment, electron attachment to electronically excited molecules, the binding of attached electrons to molecules ("electron affinity"), and the basic and the applied significance of negative-ion studies.

## Basic Electron Attachment Processes

This paper deals with negative ions formed in electron-molecule collisions at low energies ( $\approx 15$  eV). Negative ions produced at higher energies (e.g., ion-pair processes) or in collisions of molecules with electronically-excited species (e.g.,

metastable atoms, Rydberg states) will not be discussed. The basic processes to be considered, then, can be classified as electron attachment to ground state molecules, to "hot" molecules, or to electronically excited molecules.

Electron attachment to ground state molecules predominantly in their lowest state(s) of internal excitation may be represented by the scheme of Eqs. (1)-(3):

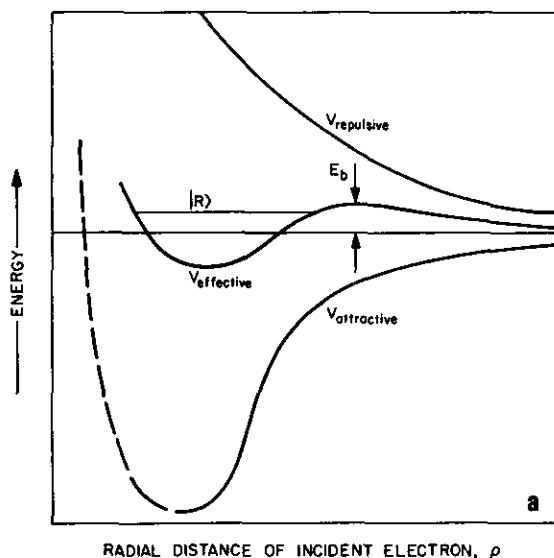
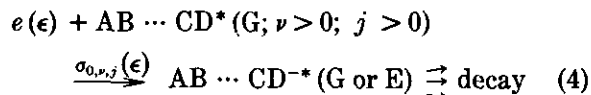


\* Atomic, Molecular and High Voltage Physics Group, Health and Safety Research Division, Oak Ridge National Laboratory, Oak Ridge, Tennessee 37830, and Department of Physics, The University of Tennessee, Knoxville, Tennessee 37916.

Here  $e(\epsilon)$  is the impacting electron of energy  $\epsilon$ ,  $AB \cdots CD(G; \nu \approx 0)$  is a neutral ground-state polyatomic molecule predominantly in its lowest vibrational,  $\nu$ , state of excitation,  $AB \cdots CD^{-*}(G \text{ or } E)$  is a transient negative ion formed in ei-

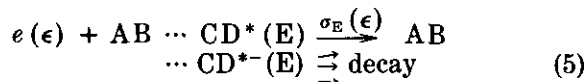
ther the field of the ground (G) or excited (E) electronic state with a capture cross section  $\sigma_0(\epsilon)$ , and  $\epsilon'(\leq \epsilon)$  is the energy of the scattered electron; the asterisk indicates excess internal energy and the asterisk in parenthesis indicates possible increase in the internal energy of the corresponding species. Reaction (1) is indirect elastic and inelastic electron scattering. Reaction (2a) is dissociative attachment leading to stable fragment negative ions (for a polyatomic molecule this process can lead to simultaneous multiple fragmentation). Reaction (2b) is dissociative attachment leading to metastable negative ion fragment(s) which are subject to autodetachment and/or autodecomposition. Reaction (3) is parent negative ion formation which is possible when the electron affinity, EA, of  $AB \cdots CD$  is positive ( $>0$  eV) and the excess internal energy is removed, principally by collision with another body. All three reactions have been studied extensively especially over the last decade. At room temperature the preponderance of  $AB \cdots CD$  molecules are in the  $\nu = 0$  level. However, depending on the molecule, even a small population of higher vibrational and/or rotational levels can affect significantly the cross sections and the onsets, especially for reaction(s) 2.

Electron attachment to "hot" molecules is summarized by Eq. (4).



Here the molecule  $AB \cdots CD^*$  is in the ground electronic state but in higher rotational,  $j$ , and/or vibrational,  $\nu$ , states. In this case the cross section for formation  $\sigma_{0,\nu,j}(\epsilon)$  and the probability of the ensuing decomposition(s) depend on the vibrational and/or rotational quantum states. Reaction (4) is appropriate to "hot" gases and it has been investigated recently.

Electron attachment to electronically excited molecules is summarized by Eq. (5).



Here the electron is captured by an electronically excited molecule with a cross section  $\sigma_E(\epsilon)$  forming  $AB \cdots CD^{*-}(E)$  in the field of an excited electronic state. Very little is known about this process.

## Modes of Electron Capture by Molecules

The various ways via which slow electrons attach to molecules have been well reviewed (1-6). In general, four such mechanisms leading to the formation of a transient negative ion [negative ion resonance (NIR)] can be distinguished: shape resonances; nuclear-excited Feshbach resonances; core-excited resonances (type I); and core-excited resonances (type II).

In Figure 1a we illustrate schematically shape resonances. Here, the electron affinity, EA, of

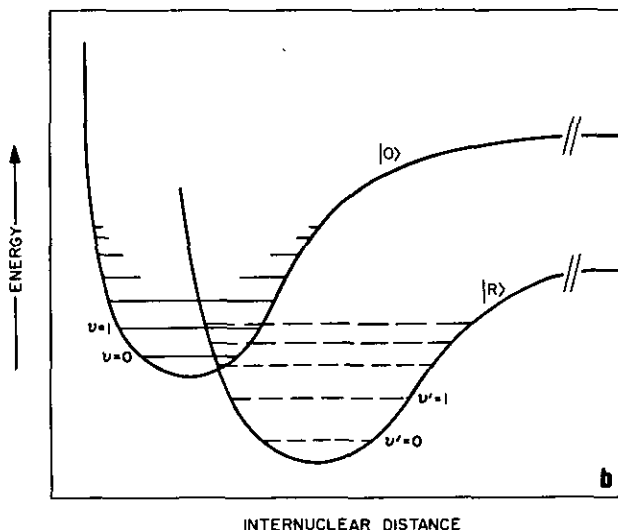


FIGURE 1. Schematic illustration of (a) shape and (b) nuclear-excited Feshbach resonances. The symbols  $|0\rangle$  and  $|R\rangle$  designate, respectively, the electronic ground state of the neutral molecule and the NIR state (5).

the molecule is negative ( $<0$  eV), and the incident electron is trapped in the potential well which arises from the interaction between the electron and the neutral molecule in its ground electronic state. This potential barrier is the combined effect ( $V_{\text{effective}}$  in Fig. 1a) of the attractive polarization potential between the neutral molecule and the incident electron ( $V_{\text{attractive}}$  in Fig. 1a) and the repulsive centrifugal potential which arises from the relative motion of the two bodies ( $V_{\text{repulsion}}$  in Fig. 1a); this latter varies as  $l(l+1)/2\rho$ , where  $l$  is the angular momentum quantum number and  $\rho$  is the electron-molecule separation. Since the negative ion potential energy curve/surface for a shape resonance lies above that of the neutral molecule, the transient ion is subject to autodetachment, decaying back to the neutral molecule in its ground electronic state plus a free electron, leaving the neutral molecule with or without vibrational and/or rotational energy. The lifetime  $\tau_a$  for this autodetachment process is a function of both the size of the barrier and the energy of the anion (i.e., the relative height and thickness of the barrier through which the electron has to penetrate). The former is strongly dependent on the  $l$  of the state occupied by the captured electron, and the latter largely on the attractive portion of the potential. If energetically possible, the NIR can undergo dissociative attachment. Such NIRs may involve an excited electronic state of the neutral molecule (i.e., electron capture is concomitant with electronic excitation of the capturing molecule) and in this case they are called core-excited (type II) resonances.

In Fig. 1b we illustrate schematically the nuclear-excited Feshbach resonance. Here EA is positive ( $>0$  eV), and the NIR lies energetically below the ground state of the neutral. Thus, unless the anion is in vibrational levels  $\nu'$  higher than the lowest vibrational level  $\nu = 0$  of the parent neutral state, the NIR cannot decay into the parent state. This mode of electron capture can involve an electronically excited neutral molecule, in which case the NIR is called core-excited (type I).

Molecular NIR states are abundant. Often they can be described [and their energies (positions) approximated] in terms of the unoccupied molecular orbitals of the neutral molecule. At times also molecular geometrical changes concomitant with electron impact and strong electrophore sites in a polyatomic molecule can constitute effective modes of electron trapping (6).

## Short-Lived Transient Negative Ions

Short-lived ( $\approx 10^{-12}$  sec) transient negative ions are a common phenomenon in low-energy electron-molecule collisions. In the incident electron energy range in which the temporal trapping of the electron occurs, the magnitude of the electron-scattering cross section changes profoundly, and the "resonance" signifies the existence and gives the position of the negative ion state. Such short-lived negative ion states—lying above the ground state of the neutral molecule—are abundant and decay by autodetachment and/or by dissociative attachment.

It is beyond the scope of this paper to discuss the theoretical treatments of NIR states of polyatomic molecules or to summarize the rather extensive recent experimental results. However, a few comments will be made on the former and a brief discussion will be given on the latter with specific reference to benzene and its substituted derivatives. For these molecules, as a rule, the  $\pi$ -electron orbitals were considered to interpret the experimental observations.

Consider, therefore, a ground state neutral molecule with  $N$  electrons forming an isolated negative ion resonance by capture of a slow electron. The captured  $[(N+1)\text{th}]$  electron normally enters an unoccupied orbital and the wavefunction  $\Psi^{N+1}$  of the resonant state resembles that of a bound state with  $N+1$  electrons. It can be expressed (1, 7, 8) as:

$$\Psi^{N+1} = \Phi^{N+1} + \int dE a(E) \phi_E^N \quad (6)$$

In Eq. (6),  $\Phi^{N+1}$  describes a bound  $(N+1)$ -electron state embedded in and degenerate with the continuum  $\{\phi_E^N; E \geq 0\}$ , and  $a(E)$  is the coefficient for the continuum. If the continuum portion of  $\Psi^{N+1}$  is neglected,

$$\Psi^{N+1} \sim \Phi^{N+1} \quad (7)$$

The (vertical) electron affinity (VEA) and the vertical attachment energy (VAE) can be approximated, respectively, by

$$\begin{aligned} \text{VEA} &\approx \langle \Psi^N | H^N | \Psi^N \rangle - \langle \Psi^{N+1} | H^{N+1} | \Psi^{N+1} \rangle \\ &= E^N - E^{N+1} \end{aligned} \quad (8a)$$

and

$$\begin{aligned} \text{VAE} &\approx \langle \Psi^{N+1} | H^{N+1} | \Psi^{N+1} \rangle - \langle \Psi^N | H^N | \Psi^N \rangle \\ &= E^{N+1} - E^N \end{aligned} \quad (8b)$$

In expressions (8a) and (8b),  $\Psi^N$  is the  $N$ -electron wavefunction for the target ground state,  $H^N$  and  $H^{N+1}$  are the corresponding Hamiltonians,

$E^N$  is the total energy (less the center of mass translation) of the  $N$ -electron ground state, and  $E^{N+1}$  is the total energy of the anion with the neutral ground state nuclear configuration. Grant and Christophorou (8) pointed out that although it is tempting to express eq. (8b) (via Koopmans' theorem) simply as

$$\text{VAE}_m \simeq E^{N+1} - E^N = \epsilon_m^N \quad (9)$$

where  $\epsilon_m^N$  is the Hartree-Fock (HF) orbital energy of the  $m$ -th unoccupied orbital of the  $N$ -electron target, a careful consideration should be given to the effects of reorganization and correlation. If  $E_{\text{reorg}}$  is the reorganization energy associated with changes in the  $N$ -electron system due to the captured electron, and  $\Delta E_{\text{corr}}$  is the change in correlation energy,

$$\text{VAE}_m = \epsilon_m^N + E_{\text{reorg}} + \Delta E_{\text{corr}} \quad (10)$$

In attempts to find out how well semi-empirical approaches explain the experimental results on the NIR states of aromatic molecules, it was found that a qualitative relationship exists between the experimental positions of the NIRs and the CNDO virtual-orbital energies for benzene and substituted benzenes (5, 8), and the theory was successful in predicting the number and relative positions of the negative ion states of these systems (5, 8-15). Semi-empirical molecular orbital methods, however, provide only a modest understanding of the shape resonances of organic molecules. They need to incorporate the effects of correlation and reorganization and to consider the  $\sigma$ -electrons along with the  $\pi$ -electron system. *Ab initio* calculations are indicated.


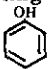

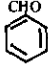


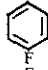
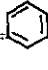
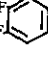
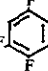
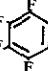
Let us now turn our attention to the experimental results on the shape resonances of benzene and substituted benzenes which can serve as a model group for other organic structures. We designate the six  $\pi$ -molecular orbitals of benzene ( $\text{C}_6\text{H}_6$ )  $\pi_1, \dots, \pi_6$ ; the three virtual (empty)  $\pi$ -molecular orbitals are  $\pi_4, \pi_5$ , and  $\pi_6$ ; in the  $D_{6h}$  and  $D_{3h}$  symmetry the orbitals  $\pi_2$  and  $\pi_3$  and  $\pi_4$  and  $\pi_5$  are degenerate. The negative ion resonances of benzene can be generally understood by considering the capture of the incident electron into the  $\pi_4, \pi_5$ , and  $\pi_6$  orbitals. Thus the observed (Table 1) NIRs of benzene were ascribed to the configurations  $\pi_1^2\pi_2^2\pi_3^2\pi_4^1$  (first NIR),  $\pi_1^2\pi_2^2\pi_3^2\pi_5^1$  (second NIR), and  $\pi_1^2\pi_2^2\pi_3^2\pi_6^1$  (third NIR) and were all characterized as shape resonances associated with the ground state molecule (the third NIR could contain an admixture of a core-excited resonance).

The introduction of a substituent onto ben-

zene breaks the degeneracy of the  $\pi_4, \pi_5$  orbitals and allows two NIRs to be observed experimentally (Table 1) as opposed to only one for benzene. The magnitude of the splitting of the first and second NIRs depends on the electronegativity of the substituent. For electron-donating substituents (e.g., F, OH,  $\text{CH}_3$ ,  $\text{NH}_2$ ) the orbital energy of the antisymmetric  $\pi$ -orbital remains virtually the same as in benzene or decreases while that of the symmetric  $\pi$ -orbital is raised relative to benzene. For electron-withdrawing substituents (e.g., CHO,  $\text{NO}_2$ , COOH) three NIRs, rather than two, were observed below  $\sim 2.5$  eV (Table 1). As indicated by Grant and Christophorou (8), in this case the antisymmetric  $\pi$ -orbital behaves essentially as described in the case of electron donating substituents, but the symmetric  $\pi$ -orbital interacts in-phase and out-of-phase with the carbonyl  $\pi^*$  orbital to split further the energies and to provide an additional resonance (see Table 1). It seems, nonetheless, that for an understanding of the NIRs of benzene, benzene derivatives, and other organic molecules one must consider the  $\sigma$ -electrons along with the  $\pi$ -electrons in both the negative ion and the neutral molecule. This can perhaps be illustrated by the recent results on the NIR states of fluorobenzenes (14) (Table 1). Frazier et al. (14) kept the substituent (F) the same but changed the number of substituents around the benzene periphery from 0 to 6. Such an increase in halogen substituents has a profound effect on the basic properties of the molecular negative ions. The electron affinity and the parent negative ion lifetime, for example, increase, the former from  $\leq 0$  eV (5) to +1.8 eV (17) and the latter from picoseconds to microseconds (6) in going from  $\text{C}_6\text{H}_6$  to  $\text{C}_6\text{F}_6$ . As expected, Frazier et al. (14) found the first and the second  $\pi$ -NIRs to be degenerate for benzene and hexafluorobenzene with  $D_{6h}$  symmetry and for 1,3,5-trifluorobenzene with  $D_{3h}$  symmetry. The energy of the lowest two NIRs is systematically lowered with increasing number of fluorine atoms (this is especially evident if one considers the weighted average position of the first and second NIR; see Table 1). The energy of the third NIR is little affected in going from  $\text{C}_6\text{H}_6$  to  $\text{C}_6\text{F}_6$ ; it is also little affected by the nature of the substituent (5, 14). This indicates that in all cases the effect of the substituent on the carbon  $p$  orbital is minimal.

On the basis of the data in Table 1, the first  $\pi$ -electron affinity of the isolated molecules of all fluorobenzenes in Table 1 is negative. As in-

Table 1. Effect of structure on the positions of the negative-ion shape resonances of benzene and some of its derivatives.<sup>a</sup>

Compound	Formula	Position of NIR (eV) <sup>b,c</sup>			
		First $\pi$ -NIR	Second $\pi$ -NIR	Third $\pi$ -NIR	$\pi^*_{CO}$
Benzene		-1.35 (-1.13) <sup>d</sup>	-1.35 (-1.13) <sup>d</sup>	-4.80 <sup>d</sup>	
Substituted benzenes with electron-donating substituents					
Phenol		-0.61 <sup>e</sup> (-1.01) <sup>f</sup>	-1.67 <sup>e</sup> (-1.73) <sup>f</sup>	-4.92 <sup>f</sup>	
Aniline		-0.55 <sup>e</sup> (-1.13) <sup>f</sup>	-1.88 <sup>e</sup> (-1.72) <sup>f</sup>	-5.07 <sup>f</sup>	
Substituted benzenes with electron-accepting substituents introducing additional NIR states					
Benzaldehyde		-0.71 <sup>e</sup>	-1.12 <sup>e</sup>	-4.61 <sup>g</sup>	-2.22 <sup>e</sup>
Benzoic Acid		-0.63 <sup>e</sup>	-1.33 <sup>e</sup>	$\leq -4.4^h$	-2.64 <sup>e</sup>
Fluorobenzenes					
Fluorobenzene		-0.91 (-0.82) <sup>d</sup>	-1.40 <sup>d</sup>	-4.66 <sup>d</sup>	
<i>p</i> -Difluorobenzene		-0.62 (-0.53) <sup>d</sup>	-1.41 <sup>d</sup>	-4.51 <sup>d</sup>	
1,3,5-Trifluorobenzene		-0.77 <sup>d</sup>	-0.77 <sup>d</sup>	-4.48 <sup>d</sup>	
2,3,5,6-Tetrafluorobenzene		-0.50 (-0.34?) <sup>d</sup>	-1.29 <sup>d</sup>	-4.51 <sup>d</sup>	
Pentafluorobenzene		-0.36 <sup>d</sup>	-1.19 <sup>d</sup>	-4.53 <sup>d</sup>	
Hexafluorobenzene		-0.42 <sup>d</sup>	-0.42 <sup>d</sup>	4.50 <sup>d</sup>	

<sup>a</sup> The position of the lowest negative ion state (traditionally referred to as the electron affinity, EA) for some of the molecules in this table are known to be positive ( $>0$  eV), i.e., the lowest negative ion state lies energetically below the first  $\pi$ -NIR listed. The EA of  $C_6H_5CHO$  and  $C_6F_6$  for example, have been reported (16, 17) to be  $\sim +0.42$  eV and  $+1.8$  eV, respectively.

<sup>b</sup> The vertical position of the NIRs is given. When available, the transition energies from the lowest vibrational level,  $v = 0$ , of the neutral molecule to the lowest vibrational level,  $v' = 0$ , of the negative ion is given in parentheses and can be considered to give the adiabatic value of EA.

<sup>c</sup> The first three NIRs are associated with the three unoccupied  $\pi$  orbitals. The  $\pi^*_{CO}$  is associated with an additional orbital resulting from an interaction of the carbonyl  $\pi^*$  orbital with one (symmetric) of the two lowest degenerate  $\pi$  orbitals of benzene. The lowest two NIRs for benzene, 1,3,5-trifluorobenzene, and hexafluorobenzene are degenerate (see text).

<sup>d</sup> Data of Frazier et al. (14).

<sup>e</sup> Data of Christophorou et al. (9).

<sup>f</sup> Data of Jordan et al. (18).

<sup>g</sup> Data of Jordan and Burrow (13).

<sup>h</sup> On the basis of the data in Table II of Frazier et al. (14).

dictated above, however, the electron affinity of  $C_6F_6$  is positive ( $+1.8$  eV) and the parent ion  $C_6F_6^{-*}$  is long-lived ( $\tau_a \approx 12 \mu\text{sec}$ ) and is formed with a large cross section at thermal electron

energies (19). This would imply either that the lowest negative ion state of  $C_6F_6$  (and perhaps of  $C_6HF_5$ ) is not a  $\pi$  but a  $\sigma$ , as suggested by Yim and Wood (20) from their electron spin

resonance work in the liquid phase, or that it is associated with a molecular distortion. The former seems to be a more likely possibility and the involvement of the  $\sigma$ -electron network is thus indicated.





For the purpose of illustrating the effect of molecular structure on the position of the shape resonances of polyatomic molecules, we now draw attention to the experimental data selected in Table 2. These indicate that the presence of a double bond lowers the position of the NIR (i.e., it increases EA). The presence of an additional double bond further lowers the position of the NIR, but this lowering is a function of the distance between the two double bonds. It is evident from the data in Table 2 that the replacement of an H atom by a  $\text{CH}_3$  group raises the NIR (lowers EA). For both aliphatic (Table 2) and aromatic (Table 1) molecules, replacement of an H atom by an electron withdrawing group (or a halogen) lowers the position of the NIR. This lowering increases with

increasing number of electron withdrawing groups (or halogens) so that EA eventually becomes  $>0$  eV and long-lived parent negative ions can form principally by a nuclear-excited Feshbach resonance mechanism. It is thus seen that, by changing the number and the position of double bonds, especially by changing the number and the nature of the substituent(s) to a basic structure (ethylene in Table 2, benzene in Table 1), NIRs can be found to occur anywhere in the subexcitation energy region.

## Dissociative Electron Attachment to Ground-State Molecules

As indicated above, resonant dissociative electron attachment is visualized to proceed through a negative ion intermediate—formed by capture of an electron in a restricted energy range defined by a Franck-Condon transition between the initial (neutral molecule and electron at infinite separation) and the final state represent-

Table 2. Effect of structure on the position of the negative-ion shape resonances of polyatomic molecules.

Molecule	Formula	Position of NIR, eV <sup>a</sup>	
		First NIR	Second NIR
Ethane	$\text{H}_3\text{C} - \text{CH}_3$	$\sim -2.3^b$	
Ethylene	$\text{H}_2\text{C} = \text{CH}_2$	$-1.78 (-1.55)^c$	
Propene	$\text{CH}_3\text{HC} = \text{CH}_2$	$-1.99^c$	
<i>Cis</i> -butene	$\text{CH}_3\text{HC} = \text{CHCH}_3$	$-2.22^c$	
1,3-Butadiene	$\text{H}_2\text{C} = \text{CH} - \text{CH} = \text{CH}_2$	$-0.62 (-0.62)^c$	$-2.80^c$
Formaldehyde	$\text{H}_2\text{C} = \text{O}$	$-0.7^d (-0.65)^e$	
Acetaldehyde	$\text{H}_3\text{CHC} = \text{O}$	$-1.3^d, -1.2^f$	
Acetone	$(\text{H}_3\text{C})_2\text{C} = \text{O}$	$-1.5^{d,f}$	
Cyclohexene		$-2.07^d$	
1,3-Cyclohexadiene		$-0.80 (-0.80)^c$	$-3.43^c$
1,4-Cyclohexadiene		$-1.75 (-1.75)^c$	$-2.67^c$
1,5-Cyclooctadiene		$-1.83^c$	$-2.33^c$
Ethylene	$\text{H}_2\text{C} = \text{CH}_2$	$(-1.55)^c$	Isoelectronic sequence; replace $\text{CH}_2$ by united atom equivalent, 0
Formaldehyde	$\text{H}_2\text{C} = \text{O}$	$(-0.65)^c$	
Oxygen	$\text{O}_2$	$(+0.44)^g$	
Ethylene	$\text{H}_2\text{C} = \text{CH}_2$	$(-1.55)^c$	
Tetracyanoethylene	$(\text{CN})_2\text{C} = \text{C}(\text{CN})_2$	$(+2.88)^g$	
Tetrachloroethylene	$\text{Cl}_2\text{C} = \text{CCl}_2$	$(+2.12)^g$	

<sup>a</sup> The uncertainty in the energy position is usually  $\pm 0.1$  eV; the values listed are vertical except those in parentheses which are adiabatic (see respective footnote in Table 1).

<sup>b</sup> Data of Pisanias et al. (21).

<sup>c</sup> Data of Jordan et al. (22).

<sup>d</sup> Data of van Veen et al. (24).

<sup>e</sup> Data of Burrow and Mischejda (23).

<sup>f</sup> Data quoted by Jordan and Burrow (13).

<sup>g</sup> Equated to the electron affinity, EA, of the molecule, and thus to the position of the lowest NIRs which can be a shape resonance or a nuclear-excited Feshbach resonance; EA values:  $\text{O}_2$  (25),  $(\text{CN})_2\text{C} = \text{C}(\text{CN})_2$  (26),  $\text{Cl}_2\text{C} = \text{CCl}_2$  (27).

ing the transient negative ion—which dissociates into (often multiple) neutral and negative-ion fragments. The reaction had been studied extensively in recent years both experimentally and theoretically. In this section we elaborate briefly on certain aspects of this most interesting process.

The cross section,  $\sigma_{da}(\epsilon)$ , for dissociative attachment as a function of electron energy,  $\epsilon$ , is equal to the product of the cross section,  $\sigma_0(\epsilon)$ , for capture of the electron by the molecule to form the metastable negative ion intermediate and the probability,  $p(\epsilon)$ , that the transient negative ion will decay via dissociative attachment (rather than via autodetachment or the other possible decay channels), viz.,

$$\sigma_{da}(\epsilon) = \sigma_0(\epsilon) p(\epsilon) \quad (11)$$

Expressions for  $\sigma_0(\epsilon)$  and  $p(\epsilon)$  have been given for diatomic molecules. Following O'Malley (28) we write for  $\sigma_{da}(\epsilon)$  for a diatomic molecule AX initially in its lowest vibrational level ( $\nu = 0$ ) and with a purely repulsive negative ion state (Fig. 2):

$$\sigma_{da}(\epsilon)_{\nu=0} = \underbrace{\frac{4\pi^{3/2}\bar{g}}{(2m/\hbar^2)\epsilon} \frac{\Gamma_a}{\Gamma_d} \exp\left\{-\frac{\Gamma_a^2 - 4(\bar{\epsilon}_0 - \epsilon)^2}{\Gamma_d^2}\right\}}_{\sigma_0(\epsilon)} \underbrace{e^{-p(\epsilon)}}_{p(\epsilon)} \quad (12)$$

In Eq. (12)  $m$  is the electron mass,  $\hbar$  is Planck's constant divided by  $2\pi$ ,  $\bar{g}$  is a statistical factor,  $\Gamma_a$  is the total autodetachment width,  $\Gamma_a$  is the partial auto-detachment width,  $\Gamma_d$  is the dissociative attachment resonance width,  $\bar{\epsilon}_0 = \epsilon_0 + \frac{1}{2}\hbar\omega$  (see Fig. 2),  $\epsilon_0$  is the electron energy at the peak of  $\sigma_{da}(\epsilon)$ ,  $\frac{1}{2}\hbar\omega$  is the zero-point energy and  $e^{-p(\epsilon)}$ , referred to as the survival probability, is now explicitly defined as

$$e^{-p(\epsilon)} = \exp\left\{-\int_{R_c}^{R_e} \frac{\Gamma_a(R)}{\hbar v(R)} dR\right\} \approx \exp\{-\bar{\tau}_a/\bar{\tau}_s\} \quad (13)$$

In Eq. (13),  $R_e$  is the interatomic separation at which electrons of energy  $\epsilon$  reach the negative ion state (within the Franck-Condon region; Fig. 2),  $R_c$  is the value of  $R$  at the crossing point between the negative ion  $AX^{-*}$  and the neutral molecule  $AX$  potential energy curves (for  $R > R_c$ ,  $p = 1$ ),  $v(R)$  is the relative velocity of separation of A and  $X^-$ ,

$$\bar{\tau}_s = \int_{R_c}^{R_e} dR/v(R)$$

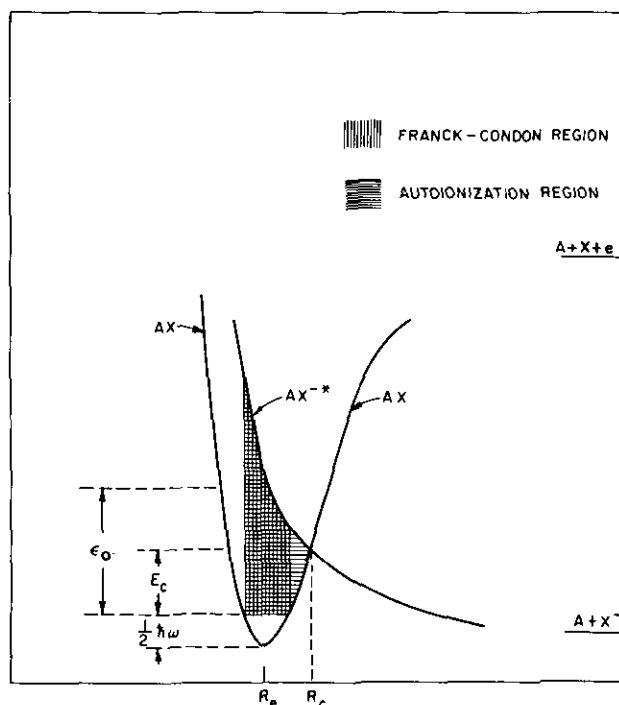


FIGURE 2. Schematic potential energy diagram illustrating the process of dissociative electron attachment for a diatomic molecule.

and

$$\bar{\tau}_a = \hbar/\Gamma_a$$

Although Eq. (12) is limited, strictly speaking, to situations as pictured in Fig. 2, it relates in a general way  $\sigma_{da}$  to  $\sigma_0$ ,  $\epsilon$ ,  $\tau_s$ ,  $\tau_a$ , and the reduced mass  $M_r$  of the A -  $X^-$  system. It explains nicely the various isotope effects observed in dissociative attachment studies (2) such as those in Figure 3 on hydrogen halides and their

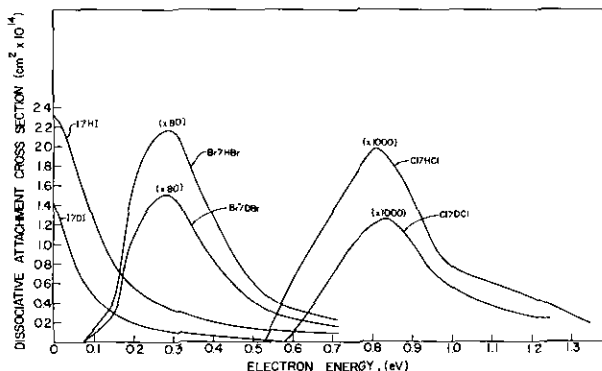


FIGURE 3. Dissociative electron attachment cross section as a function of electron energy for HCl, DCl, HBr, DBr, HI, DI, (29).

deuterated analog (29). The cross section for the deuterated analog in Fig. 3 are lower, since  $\tau_s$  is longer ( $\tau_s \propto M_r^{1/2}$ ) and the  $AX^*$  has a larger chance to decay by the competing process of autodetachment.

Negative ion potential energy curves/surfaces have a variety of shapes, and  $\sigma_{da}(\epsilon)$  is affected by these and the competitive decay channels. This limits the applicability of Eq. (12) especially in the case of polyatomic molecules. However, in certain cases of dissociative attachment to polyatomic molecules such as  $n\text{-C}_n\text{H}_{2n+1}\text{Br}$ , where the formation of  $\text{Br}^-$  involves a direct fast cleavage of  $\text{Br}^-$  along the C-Br coordinate, and the complex molecule may be visualized, as far as this process is concerned, as a diatomic-like  $\text{R}(n\text{-C}_n\text{H}_{2n+1}) - \text{Br}$  system, Eq. (12) may describe the process satisfactorily. Indeed, the relative magnitudes and the widths of the cross sections for the formation of  $\text{Br}^-$  via resonance dissociative attachment to  $n\text{-C}_n\text{H}_{2n+1}\text{Br}$  ( $n = 2$  to 6) shown in Figure 4 are consistent with their predicted dependences on the reduced masses (30). It should, of course, be noted that when  $p(\epsilon) \approx 1$ ,  $\sigma_{da}(\epsilon) \approx \sigma_0(\epsilon)$ .

In the case of polyatomic molecules, many types of fragment ions can be produced and dis-

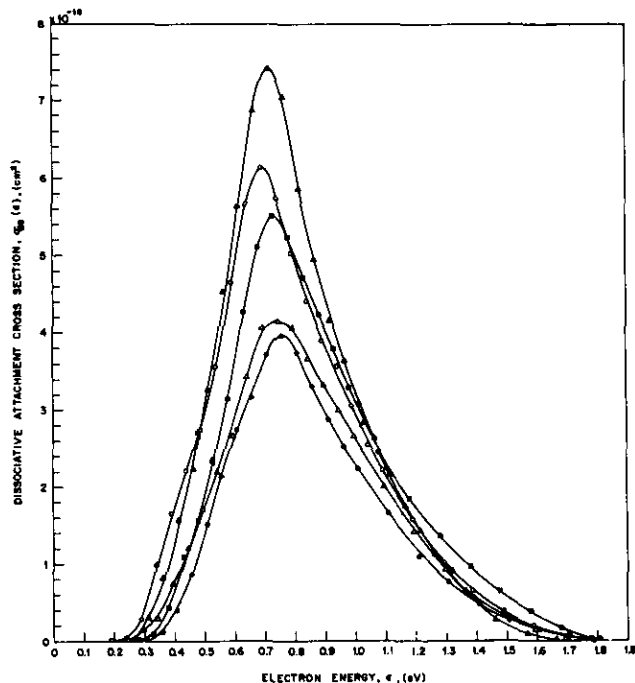


FIGURE 4. Dissociative electron attachment cross section as a function of electron energy for  $n\text{-C}_n\text{H}_{2n+1}\text{Br}$  ( $n = 2-6$ ) molecules (30): (●)  $\text{C}_2\text{H}_5\text{Br}$ ; ( $\Delta$ )  $n\text{-C}_3\text{H}_7\text{Br}$ ; (■)  $n\text{-C}_4\text{H}_9\text{Br}$ ; (○)  $n\text{-C}_5\text{H}_{11}\text{Br}$ ; ( $\blacktriangle$ )  $n\text{-C}_6\text{H}_{13}\text{Br}$ .

sociative attachment processes may not be fast; the dissociation time would depend on the distribution of the internal energy in the transient intermediate, the structural rearrangements following electron capture, and the orbital in which the electron is captured. The modes of decomposition and the nature of the fragment negative ions depend, thus, strongly on the details of molecular structure. We may identify four types of dissociative attachment fragment negative ions: directly cleaved, complementary, multiple, and rearrangement. These can be stable or metastable, subject to subsequent autodetachment and/or autodissociation.

An example of directly cleaved negative ions are the directly cleaved atomic halogen negative ions from the aliphatic hydrocarbons (Fig. 4) (30, 31), the production of which involves no internal rearrangement of the negative ion intermediate following electron capture. Additional examples are the ions  $\text{F}^-$  from  $\text{CF}_4$  and  $\text{H}^-$  from  $\text{CH}_4$  shown in Figure 5. In Figure 5 we can see also examples of complementary fragment negative ions (e.g.,  $\text{F}^-$  and  $\text{C}_3\text{F}_7^-$ , and  $\text{CF}_3^-$  and  $\text{C}_2\text{F}_5^-$  from  $n\text{-C}_3\text{F}_8$ ;  $\text{F}^-$  and  $\text{CF}_3^-$  from  $\text{CF}_4$ ), as well as examples of multiple fragment ions ( $\text{F}^-$ ,  $\text{CF}_3^-$ ,  $\text{C}_2\text{F}_5^-$ ,  $\text{C}_3\text{F}_7^-$  from  $n\text{-C}_3\text{F}_8$  since they all seem to originate from the decay of the same NIR state). It should be observed that category of complementary fragment negative ions is a special case of the category of multiple ions. This category is particularly important, in that it signifies an extensive molecular decomposition which requires concentration of internal energy in more than one coordinate.

The data collected in Figure 5 help us make a few other observations. (a) The ion  $\text{F}^-$  from  $\text{CF}_4$  and  $n\text{-C}_3\text{F}_8$ , and more generally the atomic halogen negative ion(s) from saturated aliphatic halocarbons (31) are the most abundant. Parent negative ions were not observed in electron-impact studies of the halogenated lower members of the saturated aliphatics. (b) The energy onsets and yields of complementary ions seem to show some correlation with the electron affinity of the fragments. (c) Perfluorination of a hydrocarbon lowers the positions of the negative ion states (this is supported by a large body of other information) (Table 1) (6, 14, 43). (d) The absence of  $\text{CH}_3^-$  is consistent with  $\text{EA}(\text{CH}_3) < 0$  eV. (e) From the positions of the lowest excited electronic states of  $\text{CF}_4$  and  $\text{CH}_4$  shown in Figure 5 it seems that the observed dissociative attachment resonances are associated with the ground-electronic state of  $\text{CF}_4$  and with an excited electronic state of  $\text{CH}_4$ .

Although the  $\text{F}^-$  is the predominant ion for the



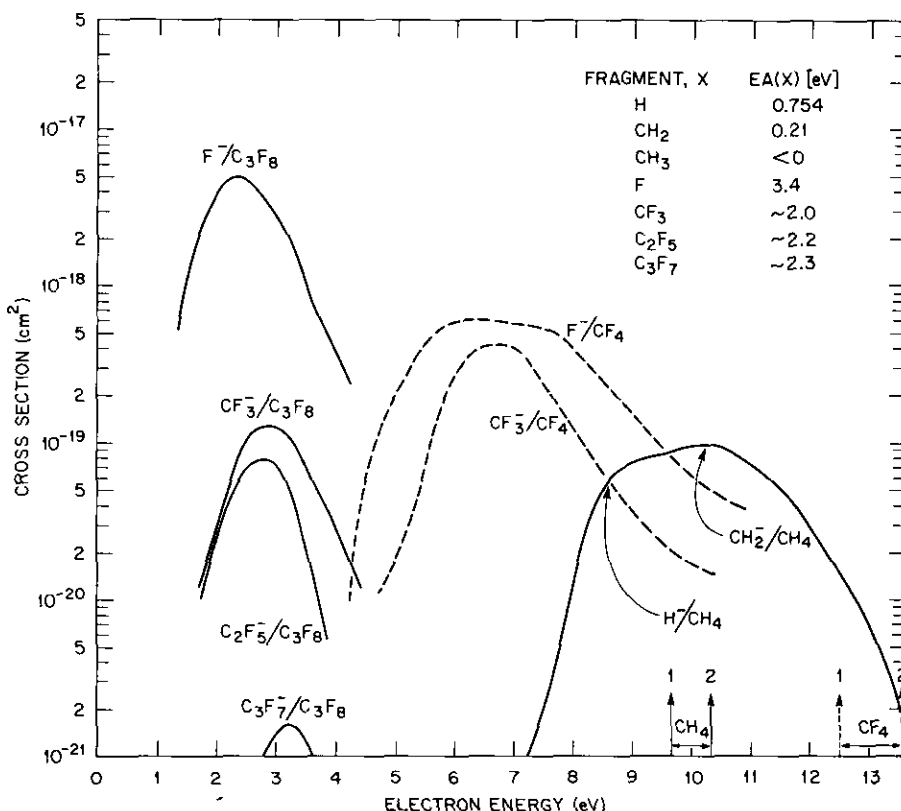


FIGURE 5. Dissociative electron attachment cross section as a function of electron energy for  $n$ -C<sub>3</sub>F<sub>8</sub>, CF<sub>4</sub> and CH<sub>4</sub>. The data plotted are from the following sources.  $n$ -C<sub>3</sub>F<sub>8</sub>: The energy dependence and the relative yield of the F<sup>-</sup>, CF<sub>3</sub><sup>-</sup>, C<sub>2</sub>F<sub>5</sub><sup>-</sup> and C<sub>3</sub>F<sub>7</sub><sup>-</sup> ions are from Lifshitz and Grajower (32). These relative cross sections were put on an absolute scale by using the value (33)  $5 \times 10^{-18}$  cm<sup>2</sup>, for the peak of the F<sup>-</sup> resonance. CF<sub>4</sub>: The energy dependence and the relative yields of the F<sup>-</sup> and CF<sub>3</sub><sup>-</sup> ions are from Lifshitz and Grajower (34). These were normalized (33) to  $6 \times 10^{-19}$  cm<sup>2</sup> at the peak of the F<sup>-</sup> resonance at ~6.2 eV. CH<sub>4</sub>: Data are from Sharp and Dowell (35). The positions of the lowest two electronic states for CH<sub>4</sub> and CF<sub>4</sub> are from Harshbarger (36) and the EA values are from: H and F (2); CH<sub>2</sub> (37); CH<sub>3</sub> (38); CF<sub>3</sub> (39,40); C<sub>2</sub>F<sub>5</sub> (42); C<sub>3</sub>F<sub>7</sub> (42).

lower members of the saturated aliphatic perfluorocarbons\*, this is not so for the unsaturated or cyclic perfluorocarbon compounds (44). For the latter, EA > 0 eV, and the parent negative ion is by far the most abundant. This can be seen from Figure 6, where the parent and fragment negative ions produced in collisions of slow electrons with perfluoro-2-butyne (2-C<sub>4</sub>F<sub>6</sub>) are shown (44). The 2-C<sub>4</sub>F<sub>6</sub> molecule is linear with freely rotating CF<sub>3</sub> groups (46). The directly cleaved F<sup>-</sup> and the complementary C<sub>3</sub>F<sub>3</sub><sup>-</sup> and CF<sub>3</sub><sup>-</sup> ions are very weak compared with the parent ion 2-C<sub>4</sub>F<sub>6</sub><sup>-</sup>. This is the case for other recently studied unsaturated and cyclic perfluorocarbons (44). Thus it is seen from Figure 7 that the parent ion of  $c$ -C<sub>4</sub>F<sub>8</sub> is

\*The parent negative ion of  $n$ -C<sub>4</sub>F<sub>10</sub> has been observed (45). No parent ion of CF<sub>4</sub>, C<sub>2</sub>F<sub>6</sub>, or  $n$ -C<sub>3</sub>F<sub>8</sub> has been reported.

much more abundant than any of the observed fragments. The F<sup>-</sup> and (M - F)<sup>-</sup> (parent molecule less one F atom)<sup>-</sup> have low yields [actually the (M - F)<sup>-</sup> ion was not observed] for  $c$ -C<sub>4</sub>F<sub>8</sub> (44), but they are the most intense ions for linear saturated aliphatic perfluorocarbons. For  $c$ -C<sub>4</sub>F<sub>8</sub> the C<sub>2</sub>F<sub>3</sub><sup>-</sup> ion, which is characterized as a rearrangement ion, was observed; its production requires geometrical changes in the transient negative ion.

All six types of fragment negative ions seem to be produced when slow electrons collide with 2-C<sub>4</sub>F<sub>8</sub> (perfluorobutene-2) (see Fig. 8): directly cleaved (e.g., F<sup>-</sup>), complementary (e.g., F<sup>-</sup>, C<sub>4</sub>F<sub>7</sub><sup>-</sup>), rearrangement (e.g., C<sub>3</sub>F<sub>5</sub><sup>-</sup>), multiple (e.g., F<sup>-</sup> and C<sub>2</sub>F<sub>3</sub><sup>-</sup> at ~5 eV; C<sub>4</sub>F<sub>7</sub><sup>-\*</sup> and C<sub>4</sub>F<sub>6</sub><sup>-\*</sup> at ~0.0 eV), metastable autodetaching (C<sub>4</sub>F<sub>7</sub><sup>-\*</sup>, C<sub>4</sub>F<sub>6</sub><sup>-\*</sup>, and C<sub>3</sub>F<sub>5</sub><sup>-\*</sup>) and, perhaps, also metastable

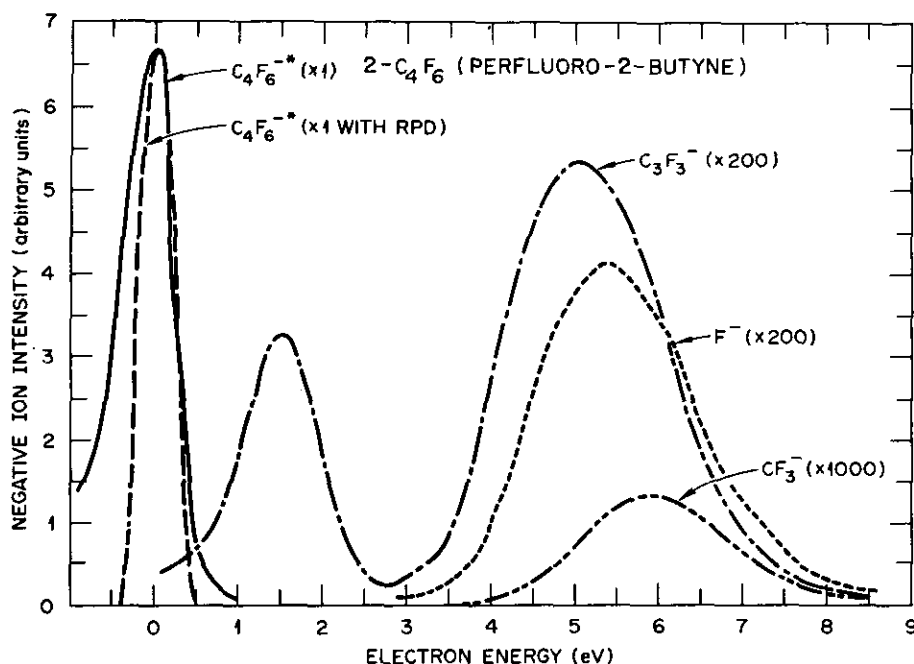


FIGURE 6. Negative ions produced by low-energy electron impact on 2-C<sub>4</sub>F<sub>6</sub> (44).

autodissociating (C<sub>3</sub>F<sub>5</sub><sup>-\*</sup>). The autodetachment lifetimes of the fragments C<sub>4</sub>F<sub>7</sub><sup>-\*</sup>, C<sub>4</sub>F<sub>6</sub><sup>-\*</sup> at ~0.0 eV and C<sub>3</sub>F<sub>5</sub><sup>-\*</sup> at ~2.3 eV were found (44) to be 7, 17, and 70 μsec, respectively; that of the parent ion C<sub>4</sub>F<sub>8</sub><sup>-\*</sup> was found to be 10 μsec at ~0.0 eV [See Christophorou (6) for a discussion of the autodetachment lifetimes of metastable parent and fragment negative ions]. The suggestion that the

C<sub>3</sub>F<sub>5</sub><sup>-\*</sup> ion is metastable both toward autodetachment and autodissociation is based on the observation that in Figure 8 the intensity of the C<sub>2</sub>F<sub>3</sub><sup>-</sup>, CF<sub>3</sub><sup>-</sup>, and C<sub>3</sub>F<sub>3</sub><sup>-</sup> ions increases when that of C<sub>3</sub>F<sub>5</sub><sup>-\*</sup> decreases. It might, thus, be possible that a fraction of the C<sub>2</sub>F<sub>3</sub><sup>-</sup>, CF<sub>3</sub><sup>-</sup> and C<sub>3</sub>F<sub>3</sub><sup>-</sup> ions is not due to the decomposition of the parent (C<sub>4</sub>F<sub>8</sub><sup>-\*</sup>) but of the fragment (C<sub>3</sub>F<sub>5</sub><sup>-\*</sup>) ion.

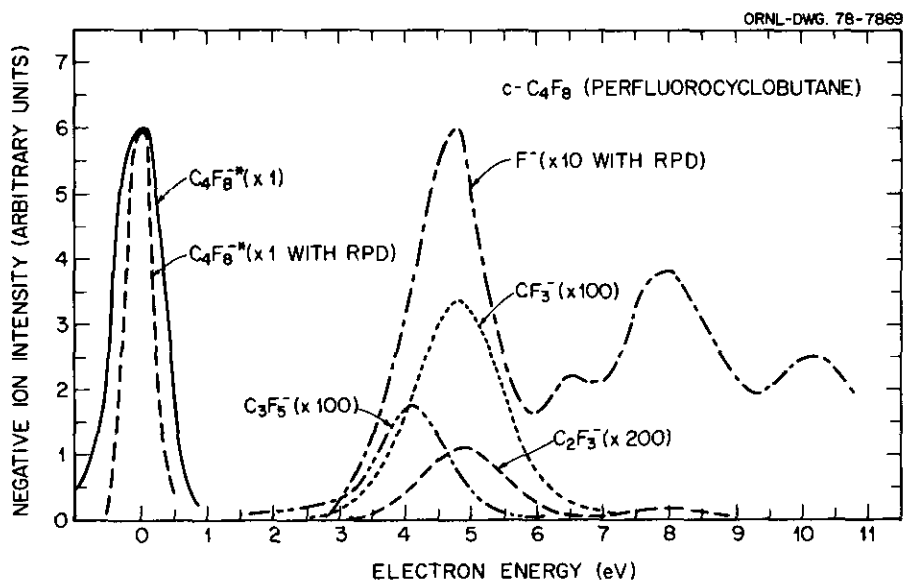


FIGURE 7. Negative ions produced by low-energy electron impact on c-C<sub>4</sub>F<sub>8</sub> (44).

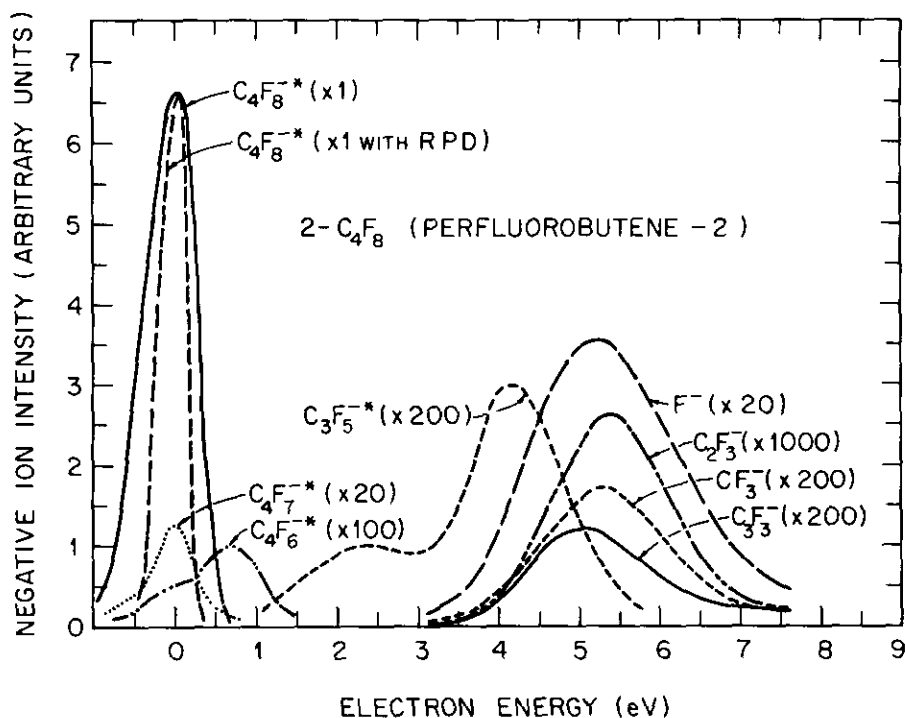


FIGURE 8. Negative ions produced by low-energy electron impact on 2-C<sub>4</sub>F<sub>8</sub> (44).

It is worth pointing out again that for cyclic and unsaturated perfluorocarbons the parent ion is the predominant ion while for saturated perfluorocarbons the predominant ion is F<sup>-</sup>. From Figures 6 to 8 and our data published elsewhere (44) it is also indicated that the fragmentation of linear and coplanar perfluorocarbons is lower compared with the cyclic and twisted compounds. This, in turn, indicates the importance of configuration and geometrical rearrangements; in this regard it is worth observing that the work of Sauers et al. (44) on 2-, 1,3-, and *c*-C<sub>4</sub>F<sub>6</sub> and 2- and *c*-C<sub>4</sub>F<sub>8</sub> indicated that double-bonded structures undergo more extensive fragmentation at low energies compared to cyclic and triple bonded systems.

The multiplicity of negative ion states and the production of a variety of negative ion fragments with large cross sections clearly show the fragility of metastable polyatomic negative ions and the effectiveness of slow (including thermal) electrons to cause extensive and often multiple molecular decompositions tantamount to a molecular "explosion." This and the delicate dependence of the type and abundance of negative ions on the details of molecular structure can, perhaps, be illustrated by the work of Johnson et al. (31) on the negative ions produced in collisions of slow ( $\leq 3$

eV) electrons with chloroethanes and chloroethylenes. For these chlorocarbons, three types of fragment negative ions were observed (31): Cl<sup>-</sup>, Cl<sub>2</sub><sup>-</sup>, and (M - Cl)<sup>-</sup> (for C<sub>2</sub>Cl<sub>4</sub> the parent ion, C<sub>2</sub>Cl<sub>4</sub><sup>-</sup>, was also observed at  $\sim 0.0$  eV and found to be metastable with an autodetachment lifetime of  $14 \pm 3$   $\mu$ sec). The Cl<sup>-</sup> ion was by far the most abundant. The intensities of the Cl<sub>2</sub><sup>-</sup> and (M - Cl)<sup>-</sup> ions with respect to Cl<sup>-</sup> depended very strongly on the number and relative positions of the Cl atoms in the molecule. The yield of Cl<sub>2</sub><sup>-</sup> was, as a rule, very much lower when the two Cl atoms in the Cl<sub>2</sub><sup>-</sup> ion originated from the same C atom. The relative cross sections for Cl<sup>-</sup> production (corrected for the finite width of the electron pulse) are shown in Figure 9 for the chloroethylenes. They indicate the existence of at least five NIRs below  $\sim 2$  eV which may be associated with orbitals dominated by the *p*-orbitals of the Cl atoms (similar results were obtained for chloroethanes) (31). Since the observed resonances in the Cl<sup>-</sup> cross-section functions seem to be associated with the Cl-atom-dominated molecular characteristics, the observed fragmentation patterns for these molecules may be common for similar bigger structures. A knowledge of the patterns of molecular decomposition(s) of halocarbons undoubtedly aids the identification of precursors of

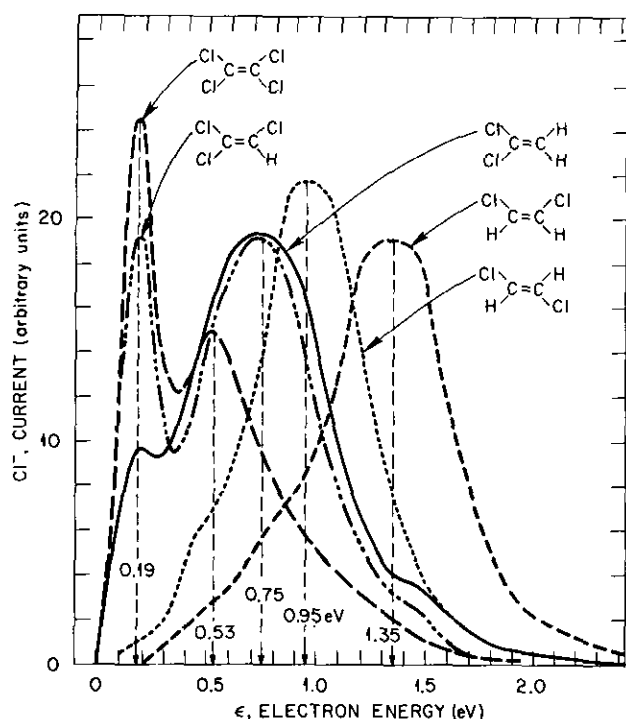


FIGURE 9.  $\text{Cl}^-$  against  $\epsilon$  for chloroethylenes (31).

atmospheric products and elucidates the reaction pathways of such pollutants in the atmosphere (2, 47).

The decomposition mechanisms responsible for specific fragment negative ions in complex molecules and the amount of translational and internal energy in the fragments depends on the decaying negative ion state and the amount and distribution of the internal energy in the excited negative ion. In spite of recent work in this area, much knowledge is still needed concerning the patterns of multiple fragmentation of molecular negative ion states and their relation to molecular structure. Of particular interest in this connection is the work of Franklin and co-workers (48-50) on the measurement of the translational energy of a number of negative (and positive) ion fragments (51). This work has shown that for a transient polyatomic molecular negative ion with  $N$  vibrational degrees of freedom only a fraction  $\alpha$  is effective, so that the sum,  $\bar{\epsilon}_i$ , of the translational energies of the fragments is

$$\bar{\epsilon}_i = E^* / \alpha N \quad (14)$$

In Eq. (14),  $E^*$  is the total excess (of the heat of the reaction) energy in the negative ion intermediate, and  $\alpha N$  may be assumed to be the number of active vibrational modes. Franklin et al. reported values of  $\alpha$  for various molecules ranging

from 0.35 to 0.57 with an average of  $\sim 0.40$ . This was taken to indicate that the effective number of vibrational degrees of freedom in the metastable intermediate is less than the available number  $N$ . Although this may be, in part, attributed to a dissociation time which is much shorter than the time for complete internal energy equilibration, it is also apparent that the effective number of vibrational degrees of freedom—and hence the value of  $\alpha$ —must depend on the spatial distribution of the wavefunction describing the orbit occupied by the captured electron. Franklin's findings on  $\alpha$  values less than one are in accord with independent work on the decomposition of transient negative ions not by autodissociation but by autodetachment (6, 54). In the latter studies basically the same model for statistical distribution of  $E^*$  was used, and although the transient negative ion considered ( $\text{C}_6\text{F}_6^-$ ) lives for  $\sim 12 \mu\text{sec}$  (6, 52) the effective number of degrees of freedom was found to be  $\sim 1/3$  of the available  $N$ .

Studies on the internal energy distribution within—and partitioning of excess energy among the decomposition products of—the transient negative ion are necessary for the deduction of accurate thermodynamic data, and the elucidation of the fragmentation processes themselves. Relevant, in this regard, is the recent conclusion of Goursaud et al. (53) that in the dissociation of triatomic negative ions, the partitioning of the excess energy favors the kinetic energy if the surface is attractive. That is, the translation to rotation-vibration coupling is weak for repulsive surfaces and strong for attractive surfaces whatever the details of the shape of the surfaces.

Finally, attention is drawn to Figure 10, where dissociative attachment cross sections as a function of electron energy are presented for a number of species in the energy range from 0 to  $\sim 16$  eV. We point out three of the salient features of the behavior of  $\sigma_{da}$ : the magnitude of  $\sigma_{da}$ —varying by more than seven orders of magnitude—depends on the position  $\epsilon_{max}$  of the NIR; the higher the  $\epsilon_{max}$  the smaller the  $\sigma_{da}$  (2, 54); as  $\epsilon_{max} \rightarrow \text{thermal}$ ,  $\sigma_{da} \rightarrow \pi \lambda^2$ ; many molecules possess a multiplicity of NIRs in the subexcitation energy region.

## Dissociative Electron Attachment to "Hot" Molecules (Effects of Temperature on Electron Attachment)

Electron attachment processes are often affected by the gas temperature  $T$ . The effects of

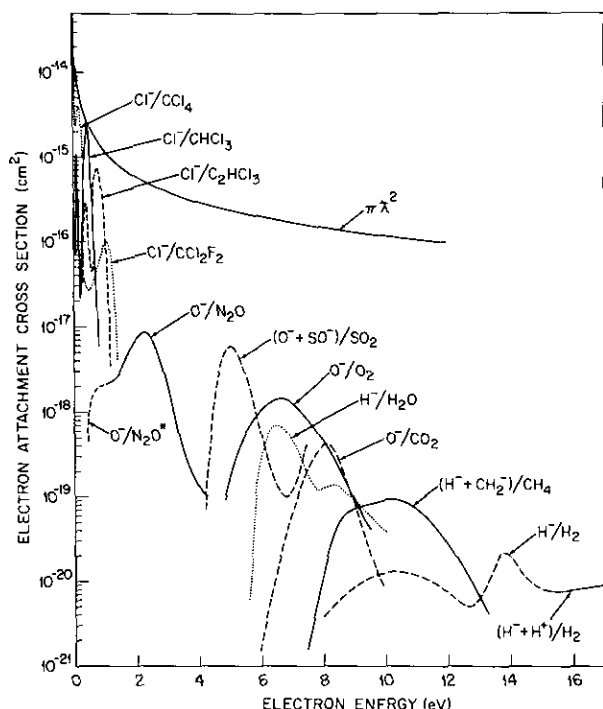


FIGURE 10. Dissociative attachment cross sections as a function of electron energy for a number of molecules. Some of the plotted  $\sigma_{da}(\epsilon)$  were deduced from swarm experiments and are thus "total" cross sections. They are identified with the specific ions as shown because these were the most abundant in mass spectrometric studies. Some of the molecules shown have other resonances which were not plotted for convenience of display.  $O^-/N_2O^*$  denotes dissociative attachment from vibrationally excited  $N_2O$  molecules, and  $(H^- + H^+)/H_2$  denotes ion pair formation from  $H_2$  (55).

temperature on the various electron attachment processes are of intrinsic value, of basic significance to determinations of thermodynamic data from electron attachment studies, and of interest to many applied areas (employing temperatures higher than ambient) where electron densities are crucially affected by negative ion formation. The effects of temperature on the magnitude and energy dependence of the cross section for specific and total negative ion production have been investigated by both the electron beam (56-63) and the electron swarm (64-69) methods; the latter have been restricted to  $T \leq 500^\circ K$ .

Let us, then, first refer to the experimental results of Fite et al. (57, 58) in Figure 11 on the temperature dependence of dissociative attachment to  $O_2$  producing  $O^-$ . It is seen from Figure 11 that as  $T$  increases, the threshold energy decreases (it actually shifts from  $\sim 4$  eV at  $\sim 300^\circ K$  to  $\sim 1.2$  eV at  $1970^\circ K$ ), the energy position of the resonance maximum decreases, and the magni-

tude of the cross section and the resonance width increase. These data have been explained theoretically by O'Malley (70), who assumed that the direct effect of  $T$  on  $O_2$  is to produce a Maxwellian distribution of vibrational ( $\nu$ ) and rotational ( $j$ ) states. The effective cross section  $\sigma_{da}(T, \epsilon)$  for dissociative attachment, then, is the Boltzmann average of the cross section  $\sigma_{da}^{\nu,j}(\epsilon)$  from each of the individual states, i.e.,

$$\sigma_{da}(T, \epsilon) = \sum_{\nu = \nu_{min}}^{\infty} \sum_{j = j_{min}}^{\infty} N \times \left| \exp \left\{ \frac{-(E_\nu + E_j)}{kT} \right\} \right| \sigma_{da}^{\nu,j}(\epsilon) \quad (15)$$

where

$$N = \left[ \sum_{\nu = \nu_{min}}^{\infty} \sum_{j = j_{min}}^{\infty} \exp \left\{ \frac{-(E_\nu + E_j)}{kT} \right\} \right]^{-1}$$

and  $\nu_{min}$  and  $j_{min}$  are subject to the energy threshold requirement

$$\epsilon + E_\nu + E_j \geq E_{threshold} = D(O-O) - EA(O) = 5.08 - 1.46 = 3.62 \text{ eV}$$

The cross section  $\sigma_{da}^{\nu,j}(\epsilon)$  is (28, 70)

$$\sigma_{da}^{\nu,j}(\epsilon) = \frac{4\pi^2 g}{k^2} \frac{\Gamma_{a,X}}{\Gamma_a} |\tilde{\chi}_\nu \left( R_\epsilon - i \frac{\Gamma_a}{\Gamma_d} \right)|^2 e^{-\nu} \quad (16)$$

where  $\tilde{\chi}_\nu$  is the vibrational wave function,  $\Gamma_{a,X}$  is the partial autodetachment width for the state  $X$ , and the rest of the symbols are as defined earlier. In his treatment, O'Malley considered the effect

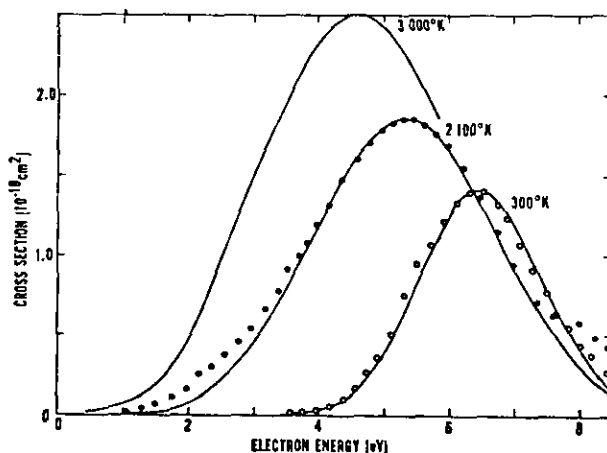


FIGURE 11. Total cross section for dissociative attachment of electrons to  $O_2$  as a function of electron energy at the indicated temperatures: (···) experimental results (57,58); (—) theoretical results (70).

of rotational states to be negligible and the excellent agreement of his predictions on the threshold, magnitude, width, and energy position of the  $O^-/O_2$  resonance with the experimental results justifies this assumption. As  $T$  increases, higher vibrational levels are populated, the internuclear distances increase (and hence the Franck-Condon region broadens) significantly and although even at 2000°K there is only a limited amount of vibrational excitation, there is a profound change in the survival factor  $e^{-\rho}$  in Eq. (16) which dominates the temperature dependence of the cross section.

The insignificance of rotational excitation seems to be at variance with earlier theoretical predictions (71) of a strong effect of rotational excitation on the yield of  $H^-/H_2$ . In this regard recent experimental (72) and theoretical (73) work on  $H^-/H_2$  in the 3.75 eV  $H_2^-$  resonance region are quite relevant. Thus the threshold cross section for the 3.75 eV  $H^-/H_2$  resonance was reported to have shown (72) an increase by a factor  $\geq 10$  with each increase in vibrational quantum and a threefold increase for rotational level increase from  $j = 0$  to  $j = 7$ . The results of a recent calculation employing resonance scattering theory with semiempirical parameters (73) shown in Table 3, indicate that although the effect of rotational excitation is not as high as that of vibrational excitation and not as significant as suggested earlier (71) it is, nonetheless, considerable.

Two additional examples can help demonstrate the effects of  $T$  on electron attachment processes. The first is on the effect of  $T$  on the production of  $O^-$  from  $N_2O$  below  $\sim 4$  eV and the second is on the effect of  $T$  on the total attachment cross section for various polyatomics.

It is seen from Figure 12 that the production of  $O^-$  from  $N_2O$  is very sensitive to  $T$  in one region (close to thermal and epithermal energies) and insensitive in another ( $\geq 2.3$  eV). It appears that two states of  $N_2O^-$  are involved in the production of  $O^-$  from  $N_2O$  below  $\sim 4$  eV. The strongly temperature sensitive portion of the cross section involves the lowest (ground) state of  $N_2O^-$  and is

Table 3. Calculated values for the  $\sigma_{da}^{vj}$  for  $H^-/H_2$  close to the 3.75 eV threshold.<sup>a</sup>

$\sigma_{da}^{vj}$ cm <sup>2</sup>	$v$	$j$
$2.8 \times 10^{-21}$	0	0
$3.5 \times 10^{-20}$	0	10
$8.3 \times 10^{-20}$	1	0
$1 \times 10^{-18}$	2	0

<sup>a</sup> Calculated by Wadehra and Bardsley (73).

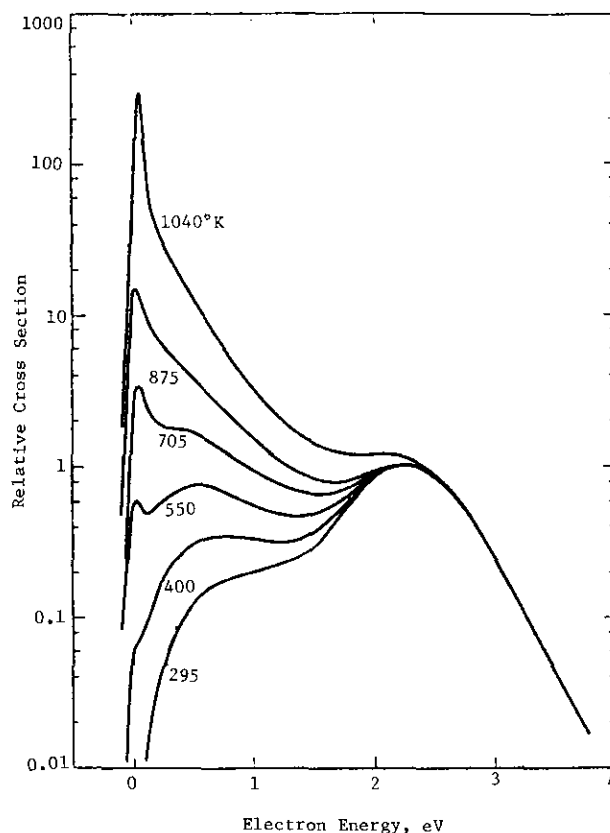


FIGURE 12. Dependence of the cross section for formation of  $O^-$  from  $N_2O$  as a function of electron energy on temperature. For all temperatures the curves were normalized at 2.25 eV; they coincide at higher energies and they differ drastically at lower energies as  $T$  changes (60).

due to excitation of the bending mode of vibration (60); it is thought to arise from the dependence of bond angle of the energy separation of the electronic ground states of  $N_2O$  and  $N_2O^-$  (the potential energy of the lowest  $N_2O^-$  state depends significantly on bond angle) (60, 66, 74). The temperature-independent peak at 2.25 eV is ascribed to dissociative attachment via the second  $N_2O^-$  state. These findings, along with those on the temperature dependence of dissociative attachment to  $O_2$ , demonstrate the significance of temperature studies in determinations of *true* onsets for specific product ions and the deduction therefrom of thermodynamic data.

In Figure 13 is shown the variation with  $T$  of the integrated total attachment cross section for various polyatomics studied by Spence and Schulz (63). Three observations can be made with respect to Figure 13: (1) the spread in the magnitude of the total attachment cross section seen at room temperature decreases as the temperature

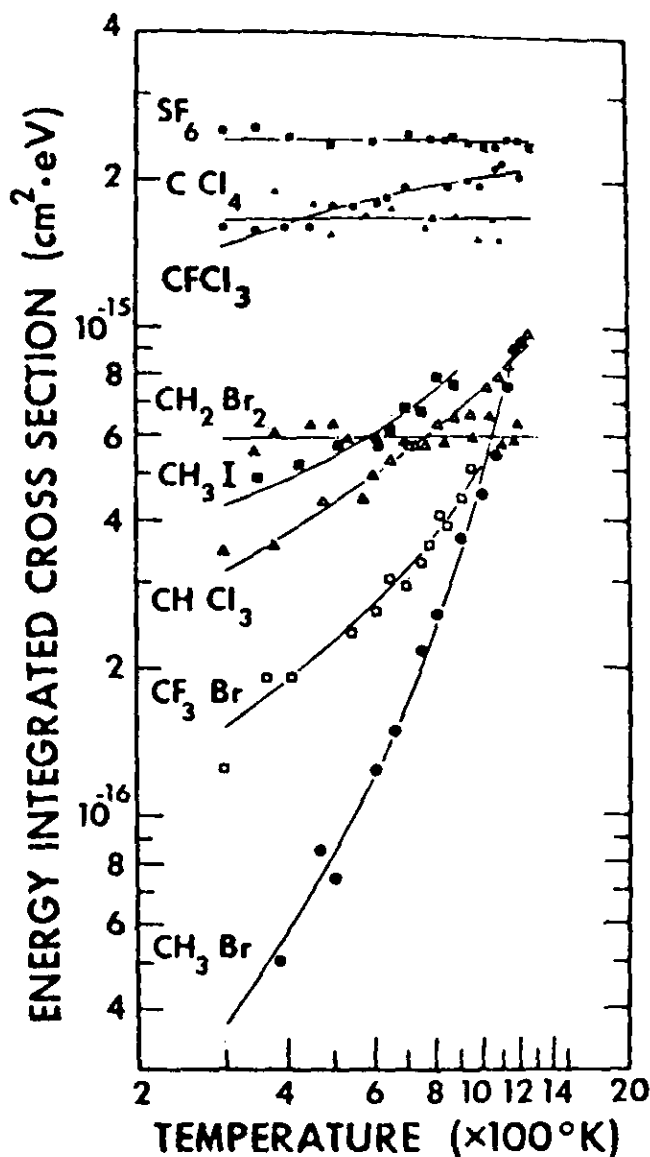


FIGURE 13. Energy integrated cross sections as a function of temperature for various halocarbons and  $\text{SF}_6$  (63).

increases; (2) the smaller the magnitude of the attachment cross section at room temperature the larger seems to be its temperature dependence; and (3) at near thermal energies the attachment cross section for polyatomics approaches the theoretical maximum value (Fig. 10) (2, 6, 55, 75, 76), which itself is insensitive to the initial vibrational state of the molecule.

### Parent Negative Ions

For a parent negative ion to form [reaction (3)], the electron affinity of the molecule must be

positive. If the excess energy of the ion  $\text{AX}^{-*}$  is not removed sufficiently fast, however, it will be destroyed by autodetachment within an average time  $\tau_a$ , even though its EA is positive. If the autodetachment lifetime,  $\tau_a$ , of the transient parent negative ion is  $\geq 10^{-6}$  sec, it can be detected in conventional time-of-flight mass spectrometers and its  $\tau_a$  can be measured (6). On the other hand, for the total pressures normally employed in swarm experiments (2, 6, 77) the time  $\tau_{\text{coll}}$  between collisions of the transient parent negative ion and a stabilizing body (usually a buffer gas molecule) (2, 77) is much smaller than  $\tau_a$ , and thus such ions are completely stabilized; swarm studies then conveniently provide  $\sigma_0(\epsilon)$  for these ions. If the transient parent negative ion is moderately long-lived (2, 6) ( $10^{-12} \leq \tau_a < 10^{-6}$  sec) its complete stabilization by collision requires very high pressure swarm experiments (2, 6, 77); these experiments can provide  $\tau_a$  and  $\sigma_0(\epsilon)$  and a great deal of information about the dynamics of electron attachment processes and the influence of the environment on them (see below). In the present section we deal briefly with long-lived and in the next with moderately long-lived parent negative ions.

The cross sections, the lifetimes, and the dependence of these two quantities on the energy of the captured electron for long-lived parent negative ions depend strongly on molecular structure. Long-lived parent negative ions are usually formed via a nuclear-excited Feshbach resonance mechanism and their cross sections are very large at thermal and epithermal electron energies (2, 6, 75, 76). The electron swarm method has been shown (2, 6, 75) to be uniquely suited for the detection of these ions and for the accurate determination of the NIR states that lead to their production along with their respective cross sections. This capability of the swarm method has been greatly enhanced by the swarm-unfolding technique (78). To illustrate these points we refer below to some recent work on perfluorinated hydrocarbons (PFHs) at the author's laboratory (75, 76, 79).

In Figure 14 the attachment cross sections,  $\sigma_a(\epsilon)$ , as a function of electron energy  $\epsilon$ , and the attachment rate,  $\alpha w(\langle \epsilon \rangle)$ , as a function of the mean electron energy  $\langle \epsilon \rangle$ , are presented for three PFHs with double and triple bonds. It is evident from these data that at least three NIR states exist below  $\sim 1.2$  eV for these molecules. The cross sections are very large compared to those of open-chain saturated PFHs with 1 to 4 carbon atoms. The latter do not attach slow electrons efficiently [see Fig. 5 for  $\text{CF}_4$  and  $n\text{-C}_3\text{F}_8$ ,

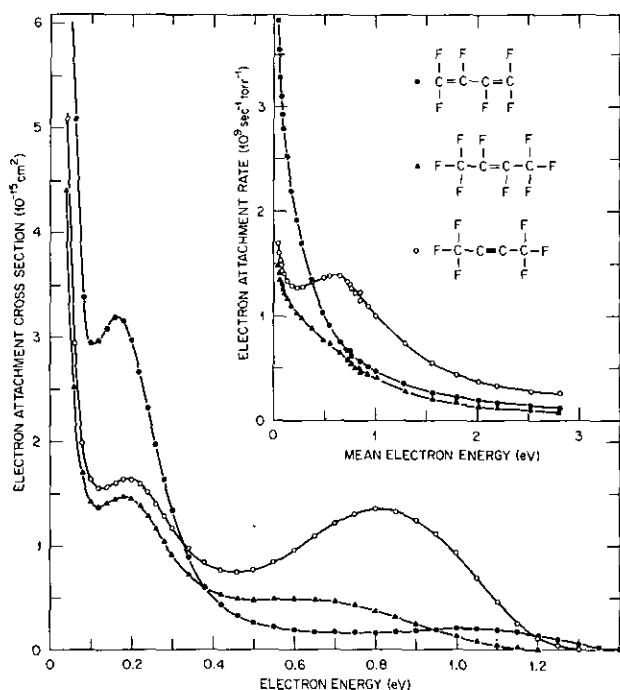


FIGURE 14. Electron attachment cross section as a function of electron energy for perfluoro-1,3-butadiene ( $1,3\text{-C}_4\text{F}_6$ ), perfluoro-2-butene ( $2\text{-C}_4\text{F}_8$ ), and perfluoro-2-butyne ( $2\text{-C}_4\text{F}_6$ ). (Inset) Electron attachment rate as a function of mean electron energy for the same compounds. Original data from Christodoulides et al. (75).

Harland and Franklin (33) for  $\text{C}_2\text{F}_6$ , and Harland and Thynne (45) for  $n\text{-C}_4\text{F}_{10}$ ], and with the exception of  $n\text{-C}_4\text{F}_{10}$  for which a very weak (intensity  $<0.1\%$  that of  $\text{F}^-$ ) parent negative ion was observed (45) no parent negative ions were reported, possibly because their electron affinities are negative.\* (The total electron attachment cross section for these PFHs increases with increasing chain length.† It is thus seen that the presence of double and triple bonds in open chain PFHs dramatically increases their electron attaching capacity. Contrary to this, the presence of double and triple bonds has little effect on the

\*It seems likely that the electron affinity of linear saturated PFHs with four or more C-atoms is positive and that the parent negative ions of these compounds are long-lived with cross sections which increase with increasing molecular size. A weak parent negative ion has been reported (45) for  $n\text{-C}_4\text{F}_{10}$ , and although Reese et al. (80) failed to observe this ion, they found that the parent negative ion of  $n\text{-C}_7\text{F}_{16}$  is very abundant (at  $\sim 0.0$  eV).

†The thermal attachment-rate constants were reported (81) to be  $<10^{-16}$ ,  $<10^{-16}$ ,  $<10^{-15}$ ,  $9.6 \times 10^{-12} \text{ cm}^3/\text{molecule-sec}$  for  $\text{CF}_4$ ,  $\text{C}_2\text{F}_6$ ,  $n\text{-C}_3\text{F}_8$ , and  $n\text{-C}_4\text{F}_{10}$ , respectively;  $c\text{-C}_3\text{F}_6$  was reported (82) also to attach thermal electrons very weakly (thermal electron attachment rate  $<3 \times 10^{-14} \text{ cm}^3/\text{molecule-sec}$ ).

magnitude of  $\sigma_a(\epsilon)$  for cyclic PFHs (compare data in Figs. 15 and 16). The cyclic structure of the latter seems to be itself the important factor in increasing their ability to attach slow electrons. This can be seen also from the data on cyclic and linear  $\text{C}_7\text{F}_{14}$  in Figure 17.

Although an increase in the size of the perfluorocarbon molecule could increase  $\sigma_a(\epsilon)$ , any such effect for the compounds in Figures 15-17 seems to be overshadowed by the much larger increase in  $\sigma_a(\epsilon)$  at near thermal energies when  $\text{CF}_3$  is substituted for F (Fig. 15;  $\text{C}_6\text{F}_6$  vs.  $\text{C}_6\text{F}_5\text{CF}_3$  in Fig. 16). For the cyclic PFHs the number of double bonds or the aromatic character of the molecule have no noticeable effect on  $\sigma_a(\epsilon)$ . From the data listed in Table 4 on the electron-attachment properties of the PFHs in Figures 15 to 17, it is apparent that for these molecules the number and the energy positions of the NIRs vary little from one structure to another in contrast to the

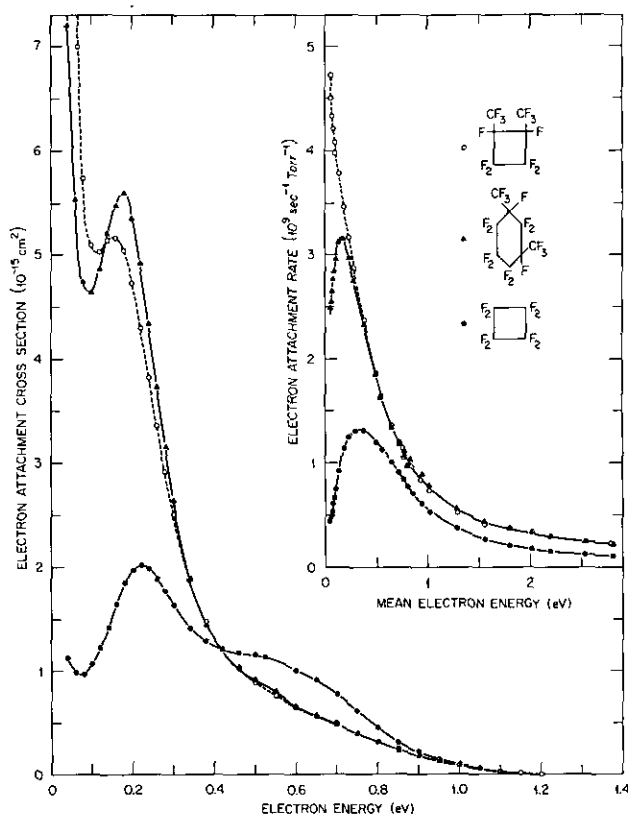


FIGURE 15. Electron attachment cross section as a function of electron energy for perfluoro-1,2-dimethylcyclobutane ( $c\text{-C}_6\text{F}_{12}$ ), perfluoro-1,3-dimethylcyclohexane ( $c\text{-C}_8\text{F}_{16}$ ), and perfluorocyclobutane ( $c\text{-C}_4\text{F}_8$ ). (Inset) Electron attachment rate as a function of mean electron energy for the same compounds. Original data from Christodoulides et al. (75) and Pak et al. (76).



large variations in the magnitude of their  $\sigma_a(\epsilon)$ . If we compare the values of the  $\sigma_a(\epsilon)$  for the PFHs in Table 4 with those of their non-fluorinated analogs it is clear that perfluorination of a hydrocarbon structure dramatically increases  $\sigma_a(\epsilon)$  at low energies. Actually the attachment cross sections and the attachment rates for the PFHs in Table 4 approach their maximum values,  $(\sigma_a)_{\max}$  and  $(\alpha w)_{\max}$ , respectively, for s-wave capture. These maximum values are shown in Fig. 16 and are defined as:

$$(\sigma_a)_{\max} = \pi\lambda^2 \quad (17)$$

and

$$[\alpha w(\langle\epsilon\rangle)]_{\max} =$$

$$N_{\text{torr}} (\pi^2 \hbar^4 / 2m^3)^{1/2} \int_0^\infty \epsilon^{-1/2} f_{N_2}(\epsilon, \langle\epsilon\rangle) d\epsilon \quad (18)$$

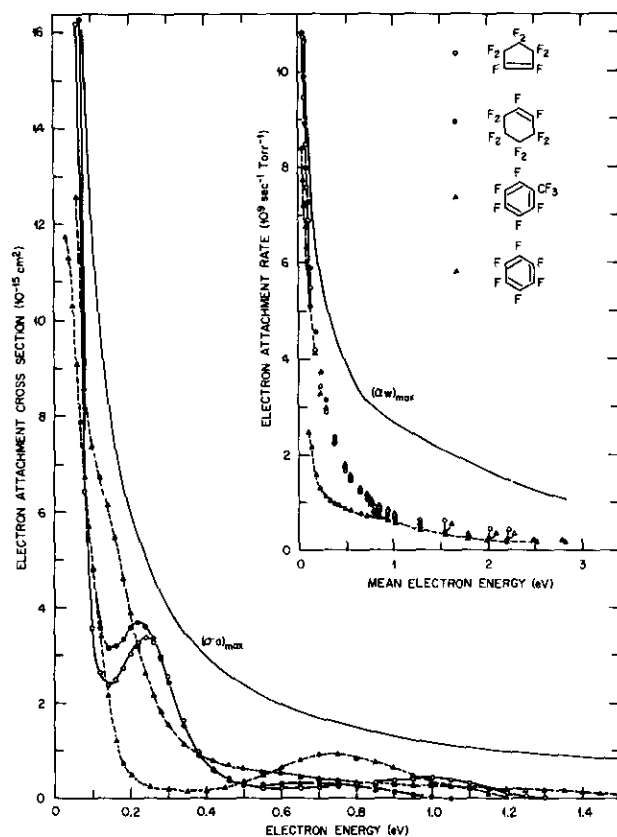


FIGURE 16. Electron attachment cross section as a function of electron energy for perfluorocyclopentene ( $c\text{-C}_5\text{F}_8$ ), perfluorocyclohexene ( $c\text{-C}_6\text{F}_{10}$ ), perfluorotoluene ( $\text{C}_7\text{F}_8$ ), and hexafluorobenzene ( $\text{C}_6\text{F}_6$ ). (Inset) Electron attachment rate as a function of mean electron energy for the same compounds. Original data from Christophorou et al. (19, 76).

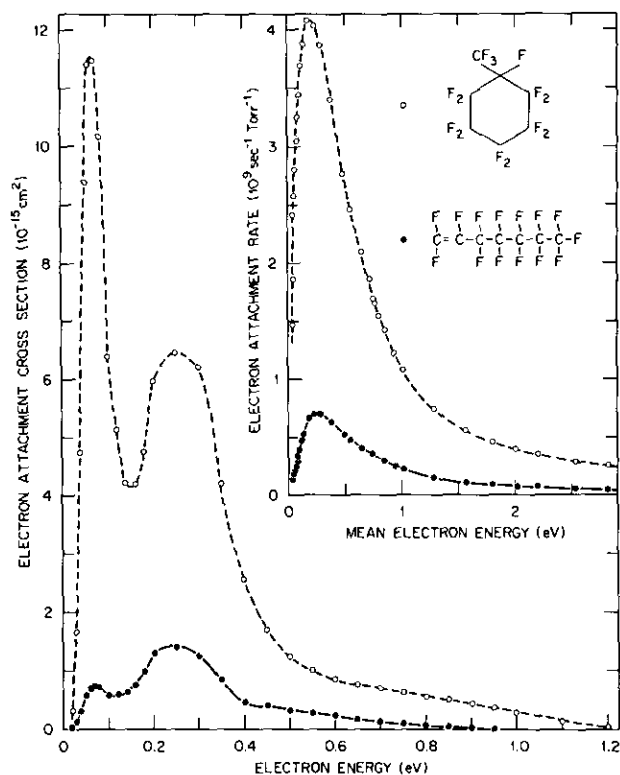


FIGURE 17. Electron attachment cross section as a function of electron energy for perfluoromethylcyclohexane ( $c\text{-C}_7\text{F}_{14}$ ) and perfluoro-1-heptene ( $1\text{-C}_7\text{F}_{14}$ ). (Inset) Electron attachment rate as a function of mean electron energy for the same compounds (79).

where  $N_{\text{torr}}$  is the number of attaching gas molecules per cubic centimeter at 1 torr pressure,  $f_{N_2}(\epsilon, \langle\epsilon\rangle)$  is the electron energy distribution function at  $\langle\epsilon\rangle$ ,  $\lambda$  is the electron de Broglie wavelength divided by  $2\pi$ , and the rest of the symbols are as defined earlier. The cross sections and the attachment rates in Figures 14 to 17 are total, i.e., for all ions produced. At thermal and near thermal energies they are mostly due to parent ions, but at higher energies (especially around the third NIR) they may contain varying degrees of contributions from dissociative attachment processes (depending on the molecule) as indicated by the electron beam studies.

A number of experimental techniques employed in electron attachment studies do not provide—as the electron swarm method of the Oak Ridge National Laboratory Group (2, 6) does—the cross section and the attachment rate as a function of electron energy, but rather only the “thermal value,”  $(\alpha w)_{\text{th}}$ , of the attachment rate. The thermal attachment rate is a strong function of the position of the NIRs and for halogenated

Table 4. Data on the electron attachment properties of perfluorocarbons.

Perfluoro-carbon	Positions of NIRs, eV	Thermal attachment rate $\times 10^{-7}$ , cm <sup>3</sup> /molecule $\times$ sec	Autodetachment lifetime of parent ion (at $\sim 0.0$ eV) $\times 10^{-6}$ , sec	Electron affinity, eV
c-C <sub>4</sub> F <sub>6</sub>	$\sim 0.0$ ; $\sim 0.14$ ; $0.71^a$	$1.5^{a,b}$ $1.4^c$	$6.9^{d,e}$ $11.2^{e,f}$	
2-C <sub>4</sub> F <sub>6</sub>	$\sim 0.0$ ; $0.19$ ; $0.80^a$	$0.55^{a,b}$	$16.3^{e,g}$ $9^f$	$>0^g$
1,3-C <sub>4</sub> F <sub>6</sub>	$\sim 0.0$ ; $0.17$ ; $1.04^a$	$1.3^{a,b}$	$7^f$	
c-C <sub>4</sub> F <sub>8</sub>	$\sim 0.0$ ; $0.22$ ; $0.48^a$	$0.12^{a,b}$ $0.09^{b,h}$ $0.11^{i,j}$ $0.12^{c,k}$ $\sim 0.2^l$	$12^{d,m}$ $6^{f,n}$ $14.8^k$ $200^{l,m}$	$\geq 0.4^n$
2-C <sub>4</sub> F <sub>8</sub>	$\sim 0.0$ ; $0.18$ ; $0.59^a$	$0.48^{a,b}$ $0.49^c$	$10^{f,n}$ $30.6^e$	$\geq 0.7^n$
c-F <sub>5</sub> F <sub>8</sub>	$\sim 0.0$ ; $0.24$ ; $0.99^p$	$3.94^{b,p}$ $1.2^j$	$26.2^{e,q}$ $50^d$	
c-C <sub>6</sub> F <sub>10</sub>	$\sim 0.0$ ; $0.22$ ; $0.71^p$	$3.99^{b,p}$ $3.13^i$	$106^{e,q}$ $113^c$	$\geq 1.4 \pm 0.3^n$
c-C <sub>6</sub> F <sub>12</sub>	$\sim 0.0$ ; $0.16^{p,q}$	$1.54^{b,p}$	$236^{e,q}$ $450^d$	
c-C <sub>8</sub> F <sub>16</sub>	$\sim 0.0$ ; $0.18^{p,q}$	$0.74^{b,p}$		
c-C <sub>7</sub> F <sub>14</sub>	$\sim 0.07$ ; $0.25^q$	$0.57^{b,q}$ $0.4^{i,j}$ $0.80^{a,k}$ $0.98^t$	$793^{d,m}$ $757^e$	
1-C <sub>7</sub> F <sub>14</sub>	$0.07$ ; $0.25^q$	$0.04^{b,q}$		
C <sub>6</sub> F <sub>6</sub>	$\sim 0.0$ ; $0.73^u$	$1.02^{v,w}$ $1.06^i$	$12^{d,u,v}$ $13.3^e$	$\geq 1.8 \pm 0.3^n$
C <sub>6</sub> F <sub>5</sub> CF <sub>3</sub>	$\sim 0.0$ ; —; $\sim 1.1^p$	$2.84^{b,p}$ $2.42^i$	$12.2^{d,m}$ $37.8^e$	$\geq 1.7 \pm 0.3^n$

<sup>a</sup> Data of Christodoulides (75).<sup>b</sup> Determined elsewhere (75) by using Eq. (19) and the  $\sigma_a(\epsilon)$  data reported in that work.<sup>c</sup> Data of Bansal and Fesenden (82).<sup>d</sup> Data of Naff et al. (43).<sup>e</sup> Data of Thynne (83).<sup>f</sup> Data of Sauers et al. (44).<sup>g</sup> Data of Hammond (84).<sup>h</sup> Data of Christodoulides (85).<sup>i</sup> Data of Davis et al. (86).<sup>j</sup> Data of Christophoron et al. (89).<sup>k</sup> Data of Harland and Thynne (87).<sup>l</sup> Data of Henis and Mabie (88).<sup>m</sup> See Christophorou (6) for discussion.<sup>n</sup> Data of Lifshitz et al. (17).<sup>p</sup> Data of Pai et al. (76).<sup>q</sup> Data of Christodoulides and Christophorou (79).<sup>r</sup> Data of Mothes et al. (90).<sup>s</sup> Data of Chen et al. (91).<sup>t</sup> Data of Mahan and Young (92).<sup>u</sup> Data of Gant and Christophorou (19).<sup>v</sup> Data of Christophorou (6).

hydrocarbons it is a strong function of the nature and number of the halogen (s) in the molecule. As can be seen from the selected data on  $(\alpha w)_{th}$  for halomethanes in Table 5,  $(\alpha w)_{th}$  increases in the order  $F < Cl < Br < I$  and with the number of the halogens in the molecule. The thermal value of  $\alpha w$  can be determined accurately when  $\sigma_a(\epsilon)$  is known from

$$(\alpha w)_{thermal} = N_{torr} (2/m)^{1/2} \int_0^\infty \epsilon^{1/2} f_M(\epsilon) \sigma_a(\epsilon) d\epsilon \quad (19)$$

where  $f_M(\epsilon)$  is a Maxwellian function characteristic of the temperature of the experiment. Values of  $(\alpha w)_{th}$  determined this way for the PFHs in Figures 14–17 are given in Table 4. In Table 4 are also listed the autodetachment lifetimes of the parent ions of these PFHs.

The time the captured electron is retained by a polyatomic molecule reveals a great deal about the interplay between the two. Knowledge of  $\tau_a$  and its dependence on the electron energy can be used as a probe of the dynamics of molecular structure and the details of the electron attachment processes. In this regard attention is drawn to the recent review by the author (6) of the autodetachment lifetimes of metastable negative ions, and to the data of Johnson et al. (102) on nitrobenzenes (Table 6). Nitrobenzenes attach strongly thermal and epithermal electrons and form long-lived parent negative ions (unless a fast dissociative attachment process effectively competes). The autodetachment lifetimes of these parent ions show an increase with increasing EA, as predicted by the theory (6). Also, they show a distinct dependence on the electron donor-acceptor properties of the substituent X and the intramolecular interaction between NO<sub>2</sub> and X. The  $\tau_a$  values for electron accepting substituents

Table 5. Thermal electron attachment rate constants for halomethanes.

Halocarbon	Rate constant, cm <sup>3</sup> /molecule-sec
CH <sub>3</sub> Cl	$<1.9 \times 10^{-15},^a <5 \times 10^{-5},^b <10^{-13}c$
CH <sub>3</sub> Br	$7 \times 10^{-12},^a 7 \times 10^{-9}d$
CH <sub>3</sub> I	$7 \times 10^{-8}e$
CH <sub>3</sub> Cl	$<1.9 \times 10^{-15},^a <5 \times 10^{-5},^b <10^{-13}c$
CH <sub>2</sub> Cl <sub>2</sub>	$4.6 \times 10^{-12},^f 4.7 \times 10^{-12},^g 4.8 \times 10^{-12},^c 1.5 \times 10^{-11}h$
CHCl <sub>3</sub>	$1.3 \times 10^{-9},^f 2.2 \times 10^{-9},^i 2.4 \times 10^{-9},^c 3.8 \times 10^{-9}h$
CCl <sub>4</sub>	$2.6 \times 10^{-7},^e 2.8 \times 10^{-7},^d,h 2.9 \times 10^{-7},^j 3.6 \times 10^{-7},^k 4.1 \times 10^{-7},^i,l$
CF <sub>4</sub>	$<10^{-16},^g \leq 10^{-16},^m <3.1 \times 10^{-13}k$
CF <sub>3</sub> Cl	$5.2 \times 10^{-14},^g <3.1 \times 10^{-13}k$
CF <sub>2</sub> Cl <sub>2</sub>	$7 \times 10^{-10},^m 1.3 \times 10^{-9},^n 1.9 \times 10^{-9},^e 2.2 \times 10^{-9},^p,g$
CFCl <sub>3</sub>	$1 \times 10^{-7},^m 1.2 \times 10^{-7},^h$

<sup>a</sup> Data of Bansal and Fessenden (93).<sup>b</sup> Data of Christodoulides et al. (94).<sup>c</sup> Data of Schultes et al. (95).<sup>d</sup> Data of Christodoulides and Christophorou (98).<sup>e</sup> Data of Christophorou (77).<sup>f</sup> Data of Christodoulides et al. (96).<sup>g</sup> Data of Fessenden and Bansal (81).<sup>h</sup> Data of Flaustein and Christophorou (97).<sup>i</sup> Data of Warman and Sauer (69).<sup>j</sup> Data of Bouby et al. (99).<sup>k</sup> Data of Davis et al. (86).<sup>l</sup> Data of Mothes et al. (90).<sup>m</sup> Data of Schumacher et al. (100).<sup>n</sup> Data of Bansal and Fessenden (82).<sup>p</sup> Data of Mothes and Schindler (101).<sup>q</sup> Data of Christophorou et al. (89).

are about ten times larger than those for electron donating substituents. Actually, CNDO calculations by Johnson et al. (102) indicated that the magnitude of  $\tau_a$  correlates with the amount of  $\pi$ -electron charge removed from the benzene ring by X when X is an electron acceptor and is little affected by the amount of  $\pi$ -electron charge donated to the benzene ring when X is an electron

donor. The large values of  $\tau_a$  for *o*-nitrophenol, *o*-nitrobenzaldehyde, and *o*-nitroaniline (Table 6) indicate the high sensitivity of  $\tau_a$  to the intramolecular interaction of NO<sub>2</sub> and X at the *ortho* position.

The measured lifetimes of long-lived parent negative ions and their dependence on  $\epsilon$ —examples of the latter are shown in Figure 18—have

Table 6. Lifetimes of long-lived parent negative ions of NO<sub>2</sub>-containing disubstituted benzene derivatives.<sup>a</sup>

Compound	Substituent, X	Lifetime $\times 10^{-6}$ , sec		
		[ <i>o</i> -XC <sub>6</sub> H <sub>4</sub> NO <sub>2</sub> ] <sup>-*</sup>	[ <i>m</i> -XC <sub>6</sub> H <sub>4</sub> NO <sub>2</sub> ] <sup>-*</sup>	[ <i>p</i> -XC <sub>6</sub> H <sub>4</sub> NO <sub>2</sub> ] <sup>-*</sup>
Nitroanisole	OCH <sub>3</sub>	16	52	10
Nitrobromobenzene	Br	18	21	10
Nitrofluorobenzene	F	17	28	10
Nitrophenol	OH	460 <sup>b,c</sup>	31 <sup>c</sup>	14 <sup>c</sup>
Nitrochlorobenzene	Cl	17	47 <sup>d</sup>	14
Nitrotoluene	CH <sub>3</sub>	13 <sup>e</sup>	19 <sup>e</sup>	14 <sup>e</sup>
Nitroaniline	NH <sub>2</sub>	46 <sup>c</sup>	21 <sup>c</sup>	15 <sup>c</sup>
Nitrobenzene	H	—	—	18 <sup>d</sup>
Nitrothiophenol	SH	—	—	23
Nitrobenzaldehyde	CHO	395	205	47
Nitrobenzoic acid	COOH	—	338	142
Nitro- $\alpha,\alpha,\alpha$ -trifluorotoluene	CF <sub>3</sub>	200	187 <sup>b</sup>	143
Nitroacetophenone	COCH <sub>3</sub>	189	310 <sup>b</sup>	196
Nitrobenzonitrile	CN	209	315 <sup>b</sup>	205
Dinitrobenzene	NO <sub>2</sub>	463	537	421

<sup>a</sup> Unless otherwise indicated the lifetime data listed are from Johnson et al. (102).<sup>b</sup> Lifetime decreases with increasing electron energy.<sup>c</sup> Data of Hadjiantoniou et al. (103).<sup>d</sup> Data of Naiff et al. (104).<sup>e</sup> Data of Christophorou et al. (105).

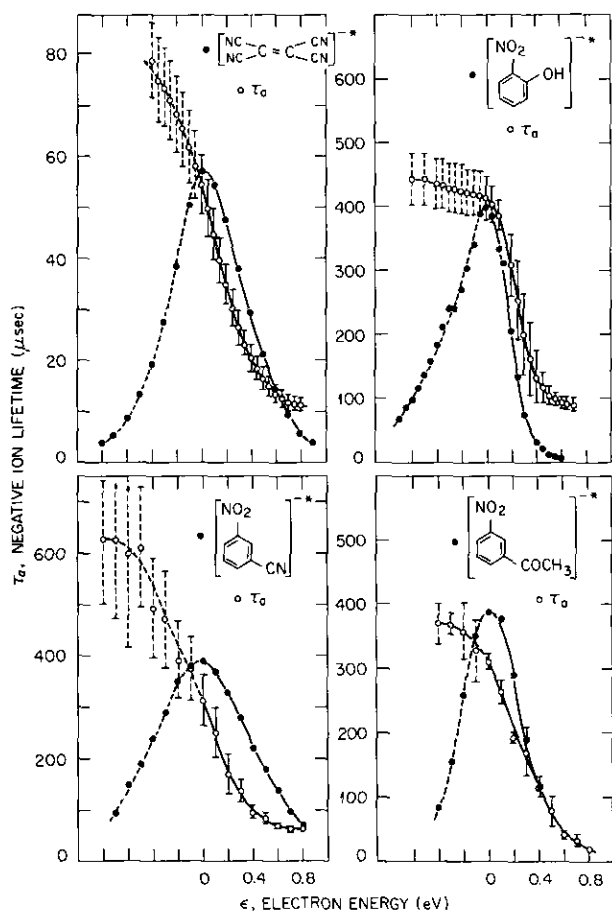


FIGURE 18. Plots of (●) negative-ion current in arbitrary units and (○) parent negative ion lifetimes as a function of electron energy for  $C_2(CN)_4$ ,  $o\text{-}C_6H_4NO_2OH$ ,  $m\text{-}C_6H_4NO_2CN$ , and  $m\text{-}C_6H_4NO_2COCH_3$  (6).

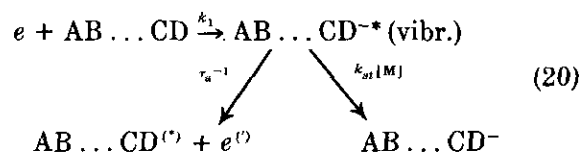
been discussed and rationalized (6) within the framework of the quasi-equilibrium theory. The theory restricts itself to the intermediate state (i.e., the transient negative ion) and does not consider in detail the entrance (initial electron capture process) and the exit (final autodetaching process) steps both of which depend strongly on selection rules and the symmetry of the state(s) involved (6). These aspects require theoretical attention.

## Effect of Density, Nature, and the State of the Medium on Electron Attachment

It has been pointed out by the author earlier that a crucial step in our efforts to link physics with chemistry and both with biology is to know how "isolated-molecule" properties change as the

molecule finds itself in gradually denser and denser gaseous and finally, in condensed-phase environments. The interfacing of the disciplines of physics, chemistry and biology requires linking physical to chemical and biological environments, i.e., it requires interphase studies.

Electron attachment to molecules and other processes and molecular properties involving separated charges, are the ones most dramatically influenced by both the density and the nature of the medium in which the electron-molecule interaction takes place. Of the electron attachment processes referred to above, the nondissociative electron attachment process involving a transient ion  $AB \dots CD^{*-}$  which requires collisional stabilization, is obviously the one (though not the only one) to show a strong dependence on the medium. Consider, then, the  $e, AB \dots CD$  system to be embedded in a gaseous medium of density  $[M]$ . The rate,  $R$ , of attachment of electrons to  $AB \dots CD$  forming  $AB \dots CD^-$  via the simple process



would be

$$R = k_1 \frac{k_{st}[M]}{\tau_a^{-1} + k_{st}[M]} \quad (21)$$

The dependence of  $R$  on  $[M]$  is a function of the relative magnitudes of  $\tau_a^{-1}$  and  $k_{st}[M]$ . If  $\tau_a^{-1} \ll k_{st}[M]$ —which is normally the case for the pressures employed in swarm experiments or when  $\tau_a > 10^{-6}$  sec— $R$  is independent of  $[M]$ . When, however,  $\tau_a^{-1} \gg k_{st}[M]$ ,  $R \propto [M]$ .

Although reaction (20) has been found to describe reasonably well the  $[M]$  dependence of  $R$  for some systems (e.g., the formation of  $O_2^-$  in  $C_2H_4$ ) over the entire density range from a few torr to the liquid density (106) in many other cases (77, 106-109) cases the formation of  $AB \dots CD^-$  depends on  $[M]$  in a complex fashion. Not only is  $M$  involved in distant collisions as a stabilizing third body but it may also be involved in the initial electron capture process affecting  $k_1$  both in magnitude and energy dependence via its effect on the negative ion states of the attaching molecules. Also, both  $\tau_a$  and  $k_{st}$  may be functions of  $\epsilon$ .

The effect of the density of a gaseous medium on the rate of attachment of electrons to molecules embedded in it can be seen from the examples in Figures 19 and 20 for, respectively,  $O_2$

in  $N_2$  (forming  $O_2^-$ ) and  $SO_2$  in  $N_2$  and  $C_2H_4$  (forming  $SO_2^-$ ). The effect of the density of the medium is a function of the nature of both the capturing species and the gaseous medium in which it is embedded as can be seen from these data and also from Figures 21 and 22, where the rate of attachment at a fixed electron energy is plotted against the density (compressibility-corrected pressure) of the medium.

Measurements, such as those in Figures 19–22, taken over a large density range can be modeled and can allow deduction of information on (1) the competitive decay channels of the metastable negative ions and their respective rate constants, (2) the lifetimes of short-lived ( $\sim 10^{-13}$ – $10^{-8}$  sec)

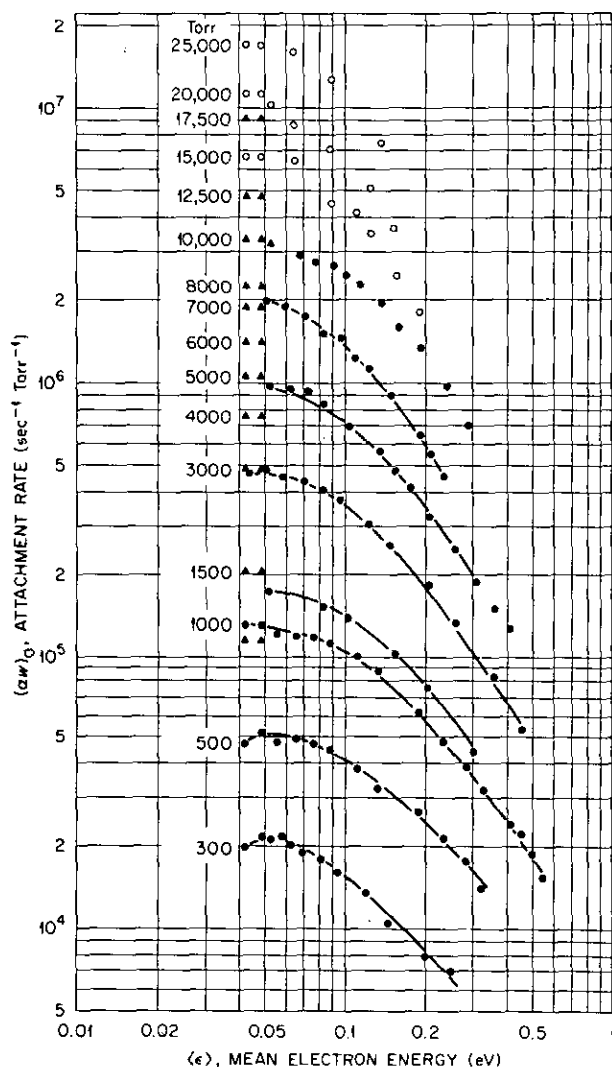


FIGURE 19. Attachment rate  $(\alpha w)_0$  as a function of mean electron energy,  $(\epsilon)$ , for  $O_2$  in  $N_2$ , for  $N_2$  pressures between 300 and 25,000 torr.  $(\alpha w)_0$  represents the measured attachment rate when  $P_{O_2} \rightarrow 0$  torr; ( $T = 298^\circ K$ ) (106).

negative ions, and (3) the rates of electron attachment to molecules at liquid-phase densities and their relation to the rates of electron attachment to molecules in liquid media.

To illustrate the first point, attention is drawn to Figure 23, where the rate,  $k_1$ , for formation of the  $C_2H_5Br^*$  ion, and the ratio of the rate constant,  $k_2$ , of dissociation of  $C_2H_5Br^*$  to the rate constant  $k_3$  of autodetachment of  $C_2H_5Br^*$  as a function of the mean electron energy  $(\epsilon)$  are plotted. For this molecule autodetachment, dissociation and stabilization of  $C_2H_5Br^*$  were assumed to proceed via a single NIR state and to be in competition (108). It is interesting to see that the autodetachment of  $C_2H_5Br^*$  predominates below and the dissociation of  $C_2H_5Br^*$  predominates above the peak of the negative-ion resonance at  $\sim 0.8$  eV.

To illustrate the second point, we list in Table 7 the lifetimes of three parent negative ions determined from such studies. No direct method is currently available for the measurement of lifetimes of negative ions shorter than  $\sim 1 \mu\text{sec}$ . The lifetimes in Table 7 were determined by assuming that the rate constant for stabilization of the transient negative ion in collisions with the molecules  $M$ , of the gaseous medium is equal to  $2\pi(e^2\alpha/M_r)^{1/2}p$ , where  $\alpha$  is the static polarizability of  $M$ ,  $e$  the electron charge,  $M_r$  the reduced mass of the negative ion and  $M$ , and  $p$  the probability of stabilization of the negative ion per collision with  $M$ . In certain cases,  $p$  is close to 1 (111) but since in general,  $p$  is likely to be  $< 1$ , the lifetimes in Table 7 are lower limits to their true values.

In connection with the third point above, the rates of attachment of thermal electrons for  $O_2$  in  $C_2H_4$ ,  $SO_2$  in  $N_2$  or  $C_2H_4$ , and  $C_6H_6$  in  $N_2$  at densities equal to those of the respective liquids, are given in Table 7. The thermal attachment rate for  $O_2$  in  $C_2H_4$  at liquid ethylene density compares well with the rate of attachment of thermal electrons to  $O_2$  in nonpolar liquids (77).

A full account of these important aspects of negative ion studies and also of the relevance and significance of electron attachment processes in gases to those in liquids can be found in the literature (77, 112–114). The involvement of vertical transitions in electron attachment to molecules dissolved in liquids in a manner analogous to that in gases is clearly indicated.

## Electron Attachment to Electronically Excited Molecules

There is virtually no information on this process [Process (5)]. To our knowledge the only

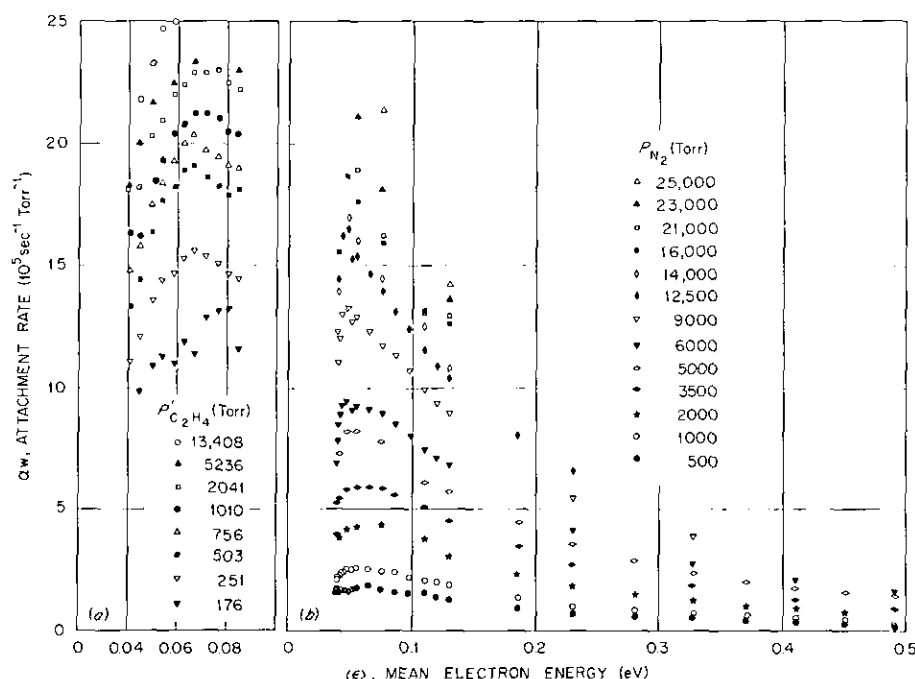
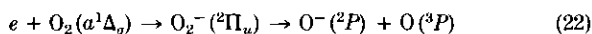
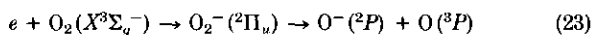


FIGURE 20. Attachment rate for  $\text{SO}_2$  in  $\text{C}_2\text{H}_4$  and in  $\text{N}_2$  as a function of the mean electron energy,  $(\epsilon)$ , at the indicated total pressures ( $T = 298^\circ\text{K}$ ) (109).

existing measurement is that of Burrow (115) on the dissociative attachment to  $\text{O}_2$  excited in the lowest (metastable)  $a^1\Delta_g$  state which lies 0.98 eV above the ground state,  $X^3\Sigma_g^-$ , of  $\text{O}_2$ . Burrow found the dissociative attachment cross section (at its maximum) for the reaction



to be  $3.5 \pm 1$  times larger than the maximum from the ground state  $\text{O}_2$ , i.e.,



Dissociative attachment to electronically excited molecules naturally have lower energy onsets and should be significant in cases where the population of low-lying metastable states is high.

## Binding of Attached Electrons to Molecules ("Electron Affinity")

The electron affinity (EA) of a molecule is normally defined as the difference in energy between the neutral molecule plus an electron at rest at infinity and the molecular negative ion when both, neutral molecule and negative ion, are in their ground electronic, vibrational, and rotational states (2). The electron affinity can be positive ( $>0$  eV) or negative ( $<0$  eV) (see Fig. 24). Two other quantities, the vertical detachment energy

(VDE) and the vertical attachment energy (VAE) are closely related to EA, the former when EA is positive and the latter when EA is negative. The VDE is defined (2) as the minimum energy required to eject the electron from the negative ion in its ground electronic and nuclear state without changing the internuclear separation, and the VAE is defined (2) as the difference in energy between the neutral molecule in its ground electronic vibrational and rotational states plus the electron at rest at infinity, and the molecular negative ion formed by addition of the electron to the neutral molecule without allowing a change in the internuclear separation of the constituent nuclei. The schematic diagrams in Figure 24 clarify the physical significance of these quantities and their relation to the various modes of electron capture discussed above.

Figures 24a, b, c refer to an electron captured in the field of the ground electronic state of an atom (Fig. 24a) and a diatomic molecule (Fig. 24b and c). In all three cases the EA is positive and the traditional measurements of EA are typical of these cases. In Figure 24a  $\text{EA}(\text{A}) = |\text{VDE}(\text{A}^-)|$ ; this is always the case for atoms. For molecules, however,  $\text{EA}(\text{AX}) = |\text{VDE}(\text{AX}^-)|$  only if the equilibrium internuclear separations for AX and  $\text{AX}^-$  are the same (as shown in Fig. 24c). Although for some small molecular species this is

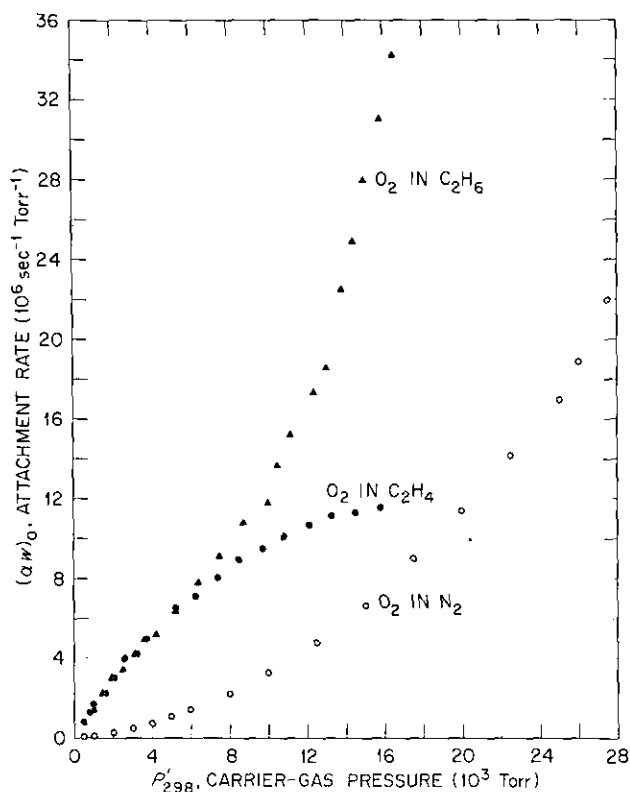


FIGURE 21. Attachment rate for  $O_2$  in the gaseous media as a function of their respective pressures: (○)  $N_2$ ; (●)  $C_2H_4$ ; (▲)  $C_2H_6$ . The data plotted are for  $\langle \epsilon \rangle \approx 0.05$  eV (106).

the case (2, 116), in the majority of molecular species a situation similar to that in Figure 24b prevails, for which  $|VDE(AX^-)| > EA(AX)$ . The cases shown in Figure 24b and c are, of course, typical examples of nuclear-excited Feshbach resonances.

Figures 24d and e illustrate the case of electron-excited Feshbach resonances (core-excited type II) for atoms and molecules, respectively. Here the electron is captured in the field of an excited atom  $A^*$  or an electronically-excited molecule  $AX^*$ , forming, respectively,  $A^{*-}$  and  $AX^{*-}$  (note our nomenclature:  $A^{*-}$  and  $AX^{*-}$  indicate, respectively, a negative ion formed by electron capture by an electronically excited atom or molecule, while  $A^{-*}$  and  $AX^{-*}$  indicate, respectively, an atomic and molecular negative ion with excess internal energy).  $EA(A^*)$  and  $EA(AX^*)$  now refer to the electron affinity of the excited atom  $A^*$  and the electronically excited molecule  $AX^*$ ; they are both positive and can be greater than those of the corresponding ground-state species. Actually the electron affinity of the ground state atom or molecule can be negative while that for the corre-

sponding excited species positive (2-4). It would be interesting to measure the vertical detachment energy  $VDE(AX^{*-})$  of  $AX^{*-}$ .

In Fig. 24f a case is depicted which is appropriate for a shape resonance. It should be noted that although in this case  $VAE(AX) \leq -EA(AX)$ , the electron is temporarily bound to the molecule with a "transient binding energy spectrum" shown by the shaded area in Figure 24f. The coordinate system depicting the potential well is indicated in the figure by  $R_{AX,e}$ , the radial distance of the electron which is different from that of the internuclear separation.

The electron affinities of atoms and molecules and the methods used for their determination have been reviewed by many authors (2, 116-119). It is apparent from these reviews and from relevant (and abundant) literature that up until the last decade EA-values were quite inaccurate. Recently, however, accurate determinations of electron affinities have become possible. It should be pointed out that depending on the sign of EA and the species, different experimental methods are appropriate and accurate. In our opinion, to date three experimental methods (see below) provide accurate values of EA, each appropriate to the specific cases exemplified in Figure 24. Equi-

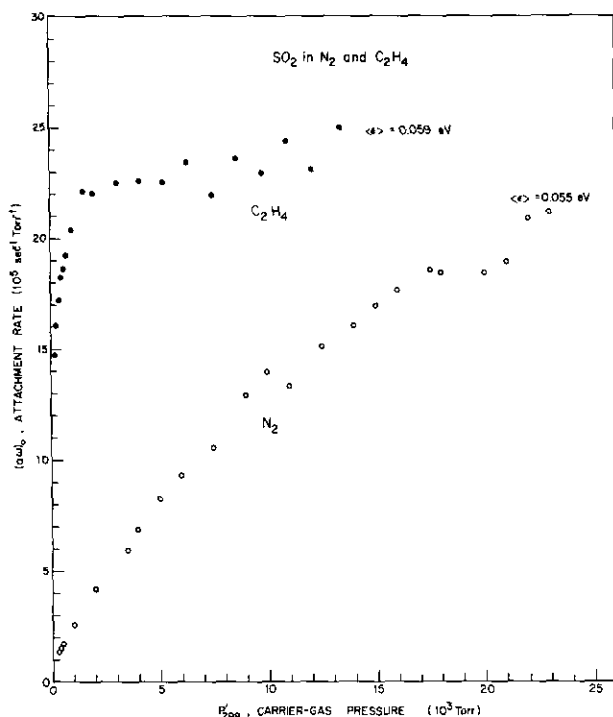


FIGURE 22. Attachment rate for  $SO_2$  (●) in  $C_2H_4$  and (○) in  $N_2$  as a function of the  $C_2H_4$  and  $N_2$  pressure for  $\langle \epsilon \rangle \approx 0.06$  eV. (109).

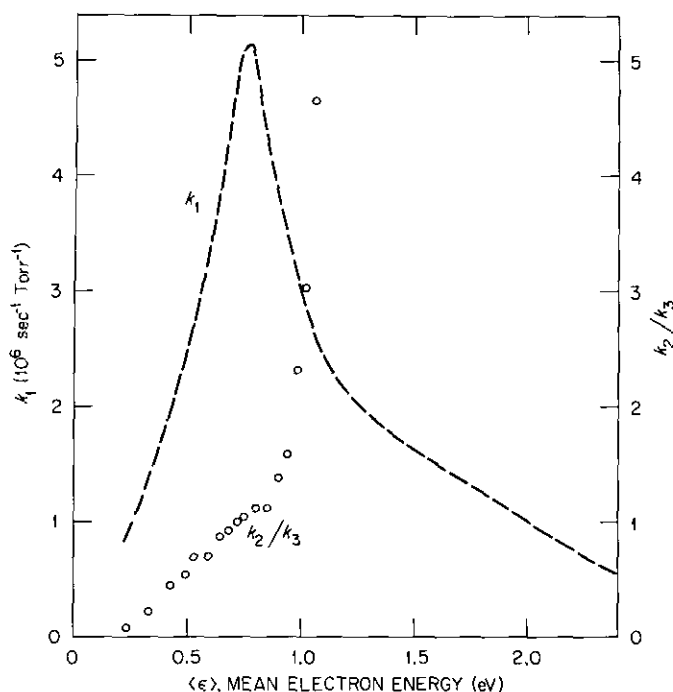


FIGURE 23.  $k_1$  and  $k_2/k_3$  as a function of  $\langle \epsilon \rangle$  for  $C_2H_5Br$ . (108).

librium methods may allow accurate determination of EA also, in cases which are free of uncertainties due to other unaccountable electron attachment processes.

## Electron Scattering Methods

These are quite accurate in providing values of the VAE and also values for the position of the  $\nu' = 0$  level of the NIR state(s), thus providing accurate (vertical and/or adiabatic) determinations of negative electron affinities (2, 4, 9-15) (Tables 1 and 2).

## Photodetachment Methods

Photodetachment methods (especially those employing laser techniques) are by far the most accurate (2, 116). Generally, these methods are restricted to the cases shown in Figure 24a and 24c, and their use to determine the electron affinity of polyatomic species (where situations such as depicted in Figure 24b are likely) is, as a rule, quite uncertain (40, 120). Recent work however, (121, 122) indicates that even for polyatomic molecules photodetachment methods can often provide accurate values of EA.

## Charge-Transfer Techniques

Charge-transfer techniques (17, 123, 124) and collisional ionization of molecules, M, using fast neutral alkali atoms, A (the EA value is deduced from the threshold of initiation of the reaction  $A^\circ + M \rightarrow A^+ + M^-$  where  $A^\circ$  is usually Na, K, Cs) seem to be most appropriate, especially the latter, for polyatomic molecules (125-128). (Proper internal energy and Doppler effect corrections are necessary for accurate determination of EA by charge-transfer technique.) Recent results on some halomethanes obtained by using alkali metal neutral atom beams are given in Table 8.

Substantial as the theoretical work has been in this area, its results, presently, lack the accuracy of the recent experimental techniques. Attention is drawn to a recent review by Simons (129).

## Basic and Applied Significance of Negative Ion Studies

Negative ion studies—encompassing a wide range of processes and novel reactions through which slow electrons and molecules embrace each other in rich and delicate ways—have attracted intense recent interest and have resulted in stimulating new advances in our knowledge of the

Table 7. Lifetimes of short-lived parent negative ions and thermal ( $T \approx 298^\circ K$ ) attachment rates for  $C_6H_6$ ,  $O_2$ , and  $SO_2$  at densities corresponding to those of liquid  $N_2$  and liquid  $C_2H_4$ .

Negative ion	Lifetime $\times 10^{-12}$ , sec <sup>a</sup>	Energy range, eV	Electron affinity, eV	Thermal attachment rate at liquid density, sec <sup>-1</sup> torr <sup>-1</sup> [sec <sup>-1</sup> M <sup>-1</sup> ]
$C_6H_6^{-*}$	1-0.2	0.04-0.18	$\sim 0$ ; $< 0^b$	$\geq 5 \times 10^4$ [ $\geq 1 \times 10^9$ ] <sup>c</sup>
$O_2^{-*}$	2	Thermal	0.44 <sup>c</sup>	$2.3 \times 10^7$ [ $4.3 \times 10^{11}$ ] <sup>f</sup>
$SO_2^{-*}$	200	Thermal	1.097 <sup>d</sup>	$2.6 \times 10^6$ [ $4.8 \times 10^{10}$ ] <sup>g</sup>

<sup>a</sup> Lower limits (see text) (77, 106).

<sup>b</sup> Data of Christophorou et al. (5, 107).

<sup>c</sup> Data of Celotta et al. (25).

<sup>d</sup> Data of Celotta et al. (110).

<sup>e</sup> From data on  $C_6H_6$  in N (400-15,000 torr) (107).

<sup>f</sup> From data on  $O_2$  in  $C_2H_4$  (750-17,000 torr) (106).

<sup>g</sup> Average of values for  $SO_2$  in  $C_2H_4$  (200-15,000 torr) and for  $SO_2$  in  $N_2$  (300-25,000 torr) (109).



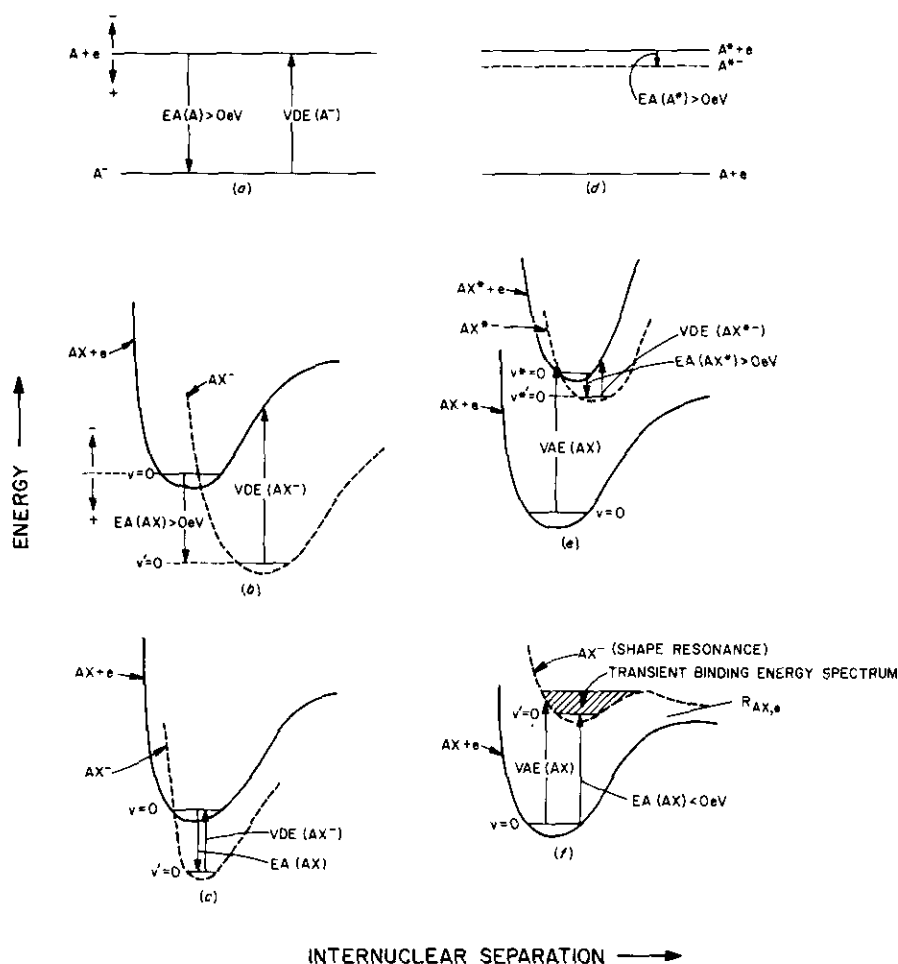


FIGURE 24. Schematic diagrams illustrating the positive and negative values of EA and the relation of EA to VAE and VDE and the modes of electron capture.

structure of matter and the interaction processes involving electrons and molecules. This is so because such studies are of unique intrinsic value and by their very nature they are trans-disciplinary covering and illuminating broad areas of physics, chemistry and biology. Of equal importance is the unique (and often direct) application they find in many fundamental areas of technology, chemical and electrical engineering, life and radiation sciences, the atmosphere and the environment.

In physics, negative ion studies provided basic knowledge on the properties of atoms and molecules, and the dynamics of electronic structure and molecular interactions. They aided the understanding of photophysical processes, the fates of electronic excitation energy, charge-transfer states and complexes. Similarly, they helped in the identification of basic reactions in upper atmosphere, space and the interaction of radiation

with matter. They contributed fundamentally to the advancement of electron physics and gaseous electronics, led to new concepts of possible practical utility such as the ion and electron lasers, and the physics of instrumentation especially in the area of radiation detectors and particle accelerators.

In chemistry, negative ion studies contributed substantially to the understanding of the quantum and electronic structure of molecules, chemical reactions, the nature of the intermediates and fast reactions in radiation chemistry. They provided a test of and a challenge for molecular orbital theory and a probe of both the gaseous and the condensed phase of matter. They yielded useful thermochemical and other data and served as the basis for a rich variety of analytical methods including those for detection, identification, quantification and removal of impurities in a variety of systems.

**Table 8. Recent electron affinity data on halomethanes and related radicals obtained by charge exchange with fast alkali atoms.<sup>a</sup>**

Molecule	Electron affinity, eV	Alkali atom
CF <sub>3</sub>	1.4 ± 0.2 <sup>b</sup>	Cs
CF <sub>3</sub> I	1.6 ± 0.2 <sup>c,d</sup>	Cs
CF <sub>3</sub> I	1.54 ± 0.2 <sup>d</sup>	Na
CF <sub>3</sub> I	2.2 ± 0.2 <sup>e</sup>	K
CF <sub>3</sub> Br	0.91 ± 0.2 <sup>d</sup>	K
CF <sub>2</sub> Cl <sub>2</sub>	0.4 ± 0.3	K
CFCl <sub>3</sub>	1.1 ± 0.3	K
CCl <sub>4</sub>	2.0 ± 0.2	K
CF <sub>3</sub>	1.9 ± 0.3	K
CF <sub>2</sub> Cl	1.6 ± 0.3	K
CFCl <sub>2</sub>	1.1 ± 0.3	K
CCl <sub>3</sub>	1.3 ± 0.3	K
CHCl <sub>2</sub>	0.0 ± 0.3	K

<sup>a</sup> The parent ions of some of these compounds were observed for the first time this way. Data of Dispert and Lacmann (128) unless otherwise noted.

<sup>b</sup> Data of Tang et al. (125).

<sup>c</sup> These authors reported EA(CH<sub>3</sub>NO<sub>2</sub>) = 0.35 ± 0.2 eV using K atoms and 0.46 ± 0.2 eV using Cs atoms.

<sup>d</sup> Data of Compton et al. (126).

<sup>e</sup> Data of MacNamee et al. (127).

In biology, negative ion studies played a basic role in clarifying the concepts used in theoretical treatments of biological action of molecules and provided key inputs to recent advances in radiation protection and sensitization, especially in the development of so-called "high affinic" drugs and radiopharmaceuticals. They have potential application in the area of biological and toxic action of molecules by properly using electron attachment processes and their products and reactions as probes of specific mechanisms and functions. They may, hopefully, lead to what we call an "electron capture-based toxicity index" for screening of toxic substances. Reactions involving parent negative ions, radicals and fragment negative ions from dissociative attachment processes, dynamics of electron capture, electron release and electron transfer and the role of these in interrupting the electron transfer cycles in the cell can all be grouped together under what we consider a potentially promising future research area which might appropriately be called bio-ionics.

In engineering and applied science, negative ion studies constitute the foundation of a wide spectrum of areas ranging from extinguishing of plasmas, arcs and flames (in this regard multicomponent gas mixtures may be properly tailored to optimize their function) to combustion and polymer construction; from radio, television, and other communications systems, space- and defense-related applications, to injection beams in

fusion machines, tornado bombing (with electron attaching gases), precipitators and health-related effects; from gas discharges to the rich and rapidly developing area of gaseous dielectrics where the concept of the multicomponent gaseous insulator shows a great promise. In most of these technological areas, it is important to realize the significance of tailoring (combining) of gases to optimize electron and ion densities (as well as electron energies) in order to enhance or to inhibit the critical reactions involved.

Finally, attention is drawn to the direct role of negative ions and their reaction processes in the rich and relatively new area of atmospheric and environmental science.

This paper reports research sponsored by the Office of Health and Environmental Research of the U.S. Department of Energy under contract W-7405-eng-26 with Union Carbide Corporation.

## REFERENCES

1. Bardsley, J. N., and Mandl, F. Resonant scattering of electrons by molecules. Repts. Progr. Phys. 31 (Part 2): 471 (1968).
2. Christophorou, L. G. Atomic and Molecular Radiation Physics, Wiley-Interscience, New York, 1971.
3. Schulz, G. J. Resonances in electron impact on atoms and diatomic molecules. Rev. Mod. Phys. 45: 378, 423 (1973).
4. Massey, H. S. W. Negative Ions, 3rd ed., Cambridge Univ. Press, Cambridge, 1976.
5. Christophorou, L. G., Grant, M. W., and McCorkle, D. L. Interactions of slow electrons with benzene and benzene derivatives. In: Advances in Chemical Physics, Vol. 36, Wiley-Interscience, New York, 1977, p. 413.
6. Christophorou, L. G. The lifetimes of metastable negative ions. In: Advances in Electronics and Electron Physics, L. Marton, Ed., Vol. 46, Academic Press, New York, 1978, p. 55.
7. Fano, U. Effects of configuration interaction on intensities and phase shifts. Phys. Rev. 124: 1866 (1961).
8. Grant, M. W., and Christophorou, L. G. On the application of molecular orbital theory to the shape resonances of organic molecules. Unpublished results.
9. Christophorou, L. G., McCorkle, D. L., and Carter, J. G. Compound-negative-ion resonant states and threshold electron excitation spectra of monosubstituted benzene derivatives. J. Chem. Phys. 60: 3779 (1974).
10. Pisanias, M. N., Christophorou, L. G., Carter, J. G., and McCorkle, D. L. Compound-negative-ion resonance states and threshold-electron excitation spectra of *N*-heterocyclic molecules: pyridine, pyridazine, pyrimidine, pyrazine and *sym*-triazine. J. Chem. Phys. 58: 2110 (1973).
11. Nenner, I., and Schulz, G. J. Temporary negative ions and electron affinities of benzene and *N*-heterocyclic molecules: pyridine, pyridazine, pyrimidine, pyrazine and *s*-triazine. J. Chem. Phys. 62: 1747 (1975).
12. Younkin, J. M., Smith, L. J., and Compton, R. N. Semi-empirical calculations of  $\pi$ -electron affinities for some conjugated organic molecules. Theoret. Chem. Acta 41: 157 (1976).
13. Jordan, K. D., and Burrow, P. D. Studies of the temporary anion states of unsaturated hydrocarbons by elec-

- tron transmission spectroscopy. *Accts. Chem. Res.* 11: 341 (1978).
14. Frazier, J. R., Christophorou, L. G., Carter, J. G., and Schweinler, H. C. Low-energy electron interactions with organic molecules: negative ion states of fluorobenzenes. *J. Chem. Phys.* 69: 3807 (1978).
15. Burrow, P. D., Michejda, J. A., and Jordan, K. D. Experimental study of the negative ion states of styrene. A test of the pairing theorem. *J. Am. Chem. Soc.* 98: 6392 (1976).
16. Wentworth, W. E., Kao, L. W., and Becker, R. S. Electron affinities of substituted aromatic compounds. *J. Phys. Chem.* 79: 1161 (1975).
17. Lifshitz, C., Tiernan, T. O., and Hughes, B. M. Electron affinities from endothermic negative-ion charge-transfer reactions. IV.  $\text{SF}_6$ , selected fluorocarbons and other polyatomic molecules. *J. Chem. Phys.* 59: 3182 (1973).
18. Jordan, K. D., Michejda, J. A., and Burrow, P. D. Electron transmission studies of the negative ion states of substituted benzenes in the gas phase. *J. Am. Chem. Soc.* 98: 7189 (1976).
19. Gant, K. S., and Christophorou, L. G. Attachment of slow electrons to hexafluorobenzene. *J. Chem. Phys.* 65: 2977 (1976).
20. Yim, M. B., and Wood, D. E. Free radicals in an adamantane matrix. XII. EPR and INDO study of  $\sigma^* \rightarrow \pi^*$  cross-over in fluorinated benzene anions. *J. Am. Chem. Soc.* 98: 2053 (1976).
21. Pisanias, M. N., Christophorou, L. G., and Carter, J. G. Threshold-electron excitation and compound negative ion formation in polyatomic molecules. Oak Ridge National Laboratory Report, ORNL/TM-3904, 1972.
22. Jordan, K. D., Michejda, J. A., and Burrow, P. D. A study of the negative ion states of selected cyclodienes by electron transmission spectroscopy. *Chem. Phys. Letters* 42: 227 (1976).
23. Burrow, P. D., and Michejda, J. A. Electron transmission study of the formaldehyde electron affinity. *Chem. Phys. Letters* 42: 223 (1976).
24. van Veen, E. H., van Dijk, W. L., and Brongersma, H. H. Low-energy electron-impact excitation spectra of formaldehyde, acetaldehyde and acetone. *Chem. Phys.* 16: 337 (1976).
25. Celotta, R. J., Bennett, R. A., Hall, J. L., Siegel, M. W., and Levine, J. Molecular photodetachment spectroscopy. II. The electron affinity of  $\text{O}_2$  and the structure of  $\text{O}_2^-$ . *Phys. Rev. A* 6: 631 (1972).
26. Farragher, A. L., and Page, F. M. Experimental determination of electron affinities. Part 11. Electron capture by some cyanocarbons and related compounds. *Trans. Faraday Soc.* 63: 2369 (1967).
27. Gaines, A. F., Kay, J., and Page, F. M. Determination of electron affinities. Part 8. Carbon tetrachloride, chloroform and hexachloroethane. *Trans. Faraday Soc.* 62: 874 (1966).
28. O'Malley, T. F. Theory of dissociative attachment, *Phys. Rev.* 150: 14 (1966).
29. Christophorou, L. G., Compton, R. N., and Dickson, H. W. Dissociative electron attachment to hydrogen halides and their deuterated analogs. *J. Chem. Phys.* 48: 1949 (1968).
30. Christophorou, L. G., Carter, J. G., Collins, P. M., and Christodoulides, A. A. Electron attachment to aliphatic hydrocarbons of the form  $n\text{-C}_n\text{H}_{2n+1}\text{Br}$  ( $n = 2-6$  and 8). II. A swarm-beam study. *J. Chem. Phys.* 54: 4706 (1971).
31. Johnson, J. P., Christophorou, L. G., and Carter, J. G. Fragmentation of aliphatic chlorocarbons under low-energy ( $\leq 10$  eV) electron impact. *J. Chem. Phys.* 67: 2196 (1977).
32. Lifshitz, C., and Grajower, R. Dissociative electron capture and dissociative ionization in perfluoropropane. *Int. J. Mass Spectrom. Ion Phys.* 3: 211 (1969).
33. Harland, P. W., and Franklin, J. L. Partitioning of excess energy in dissociative resonance capture processes. *J. Chem. Phys.* 61: 1621 (1974).
34. Lifshitz, C., and Grajower, R. Dissociative electron capture and dissociative ionization in perfluorocyclobutane. *Int. J. Mass Spectrom. Ion Phys.* 10: 25 (1972/73).
35. Sharp, T. E., and Dowell, J. T. Isotope effects in dissociative attachment of electrons in methane. *J. Chem. Phys.* 46: 1530 (1967).
36. Harshbarger, W. R., Robin, M. B., and Lassette, E. N. The electron impact spectra of the fluoromethanes. *J. Electr. Spectrom. Related Phenomena* 1: 319 (1972/73).
37. Zittel, P. F., Ellison, G. B., Oneil, S. V., Herbst, E., Lineberger, W. C., and Reinhardt, W. P. Laser photoelectron spectrometry of  $\text{CH}_2^-$ . Singlet-triplet splitting and electron affinity of  $\text{CH}_2$ . *J. Am. Chem. Soc.* 98: 3731 (1976).
38. Hush, N. S., and Pople, J. A. Ionization potentials and electron affinities of conjugated hydrocarbon molecules and radicals. *Trans. Faraday Soc.* 51: 600 (1955).
39. Dispert, H., and Lacmann, K. Negative ion formation in collisions between potassium and fluoro- and chloromethanes; electron affinities and bond dissociation energies. *Int. J. Mass Spectrom. Ion Phys.* 28: 49 (1978).
40. Richardson, J. H., Stephenson, L. M., and Brauman, J. I. Photodetachment of electrons from trifluoromethyl and trifluorosilyl ions; the electron affinities of  $\text{CF}_3^-$  and  $\text{SiF}_3^-$ . *Chem. Phys. Letters* 30: 17 (1975).
41. Richardson, J. H., Stephenson, L. M., and Brauman, J. I. Photodetachment of electrons from phenoxides and thiophenoxide. *J. Am. Chem. Soc.* 97: 2967 (1975).
42. Harland, P. W., and Thynne, J. C. J. Dissociative electron capture in perfluoropropylene and perfluoropropane. *Int. J. Mass Spectrom. Ion Phys.* 9: 253 (1972).
43. Naff, W. T., Cooper, C. D., and Compton, R. N. Transient negative-ion states in alicyclic and aromatic fluorocarbon molecules. *J. Chem. Phys.* 49: 2784 (1968).
44. Sauers, I., Christophorou, L. G., and Carter, J. G. Electron attachment to perfluorocarbon compounds. Part III. Fragmentation of aliphatic perfluorocarbons of interest to gaseous dielectrics. *J. Chem. Phys.* 71: 3016 (1979).
45. Harland, P. W., and Thynne, J. C. J. Negative-ion formation by perfluoro-n-butane as the result of low energy electron impact. *Int. J. Mass Spectrom. Ion Phys.* 11: 445 (1973).
46. Chang, C. H., Andreassen, A. L., and Bauer, S. H. The molecular structure of perfluorobutyne-2 and perfluorobutadiene-1,3 as studied by gas phase electron diffraction. *J. Org. Chem.* 36: 920 (1971).
47. Dillard, J. G. Negative ion mass spectrometry. *Chem. Rev.* 73: 589 (1973).
48. DeCorpo, J. J., Bafus, D. A., and Franklin, J. L. Correlation of excess energies of dissociative electron attachment processes with the translational energies of their products. *J. Chem. Phys.* 54: 1592 (1971).
49. Franklin, J. L. Energy partitioning in the products of ionic decomposition. *Science* 193: 725 (1976).
50. Carter, D. E. Translational energies from ionic fragmentation. *J. Chem. Phys.* 65: 2584 (1976).
51. Haney, M. A., and Franklin, J. L. Correlation of excess energies of electron-impact dissociations with the translational energies of the products. *J. Chem. Phys.* 48: 4093 (1968).
52. Christophorou, L. G., Gant, K. S., and Anderson, V. E.

- Long-lived parent negative ions formed via nuclear-excited Feshbach resonances. Part 5-. Effective number of degrees of freedom participating in the sharing of the ion's excess energy. *J. Chem. Soc. Faraday Trans. II*, 73: 804 (1977).
53. Goursaud, S., Sizun, M., and Fiquet-Fayard, F. Translational energies from triatomic negative ions fragmentation. *J. Chem. Phys.* 68: 4310 (1978).
  54. Christophorou, L. G., and Stockdale, J. A. D. Dissociative electron attachment to molecules. *J. Chem. Phys.* 48: 1956 (1968).
  55. Christophorou, L. G. Elementary electron-molecule interactions and negative ion resonances at subexcitation energies and their significance in gaseous dielectrics. In: *Proceedings of the XIIIth International Conference on Phenomena in Ionized Gases*, Berlin, 1977, Invited Lectures, pp. 51-73.
  56. Hickam, W. M., and Berg, D. Negative ion formation and electric breakdown in some halogenated gases. *J. Chem. Phys.* 29: 517 (1958).
  57. Fite, W. L., and Brackmann, R. T. Electron collisions with atomic and molecular oxygen. In: *Proceedings of the Sixth International Conference on the Ionization Phenomena in Gases*, Paris, 1963, Vol. I, p. 21.
  58. Henderson, W. R., Fite, W. L., and Brackmann, R. T. Dissociative attachment of electrons to hot oxygen. *Phys. Rev.* 183: 157 (1969).
  59. Spence, D., and Schulz, G. J. Temperature dependence of dissociative attachment in  $O_2$  and  $CO_2$ . *Phys. Rev.* 188: 280 (1969).
  60. Chantry, P. J. Temperature dependence of dissociative attachment in  $N_2O$ . *J. Chem. Phys.* 51: 3369 (1969).
  61. Chen, C. C., and Chantry, P. J. Temperature dependence of  $SF_6^-$ ,  $SF_5^-$  and  $F^-$  production from  $SF_6$ . *Bull. Am. Phys. Soc.* 15: 418 (1970).
  62. Chen, C. C., and Chantry, P. J. Dissociative attachment of low energy electrons in  $CCl_2F_2$  and  $CHClF_2$ . *Bull. Am. Phys. Soc.* 17: 1133 (1971).
  63. Spence, D., and Schulz, G. J. Temperature dependence of electron attachment at low energies for polyatomic molecules. *J. Chem. Phys.* 58: 1800 (1973).
  64. Compton, R. N., Christophorou, L. G., Hurst, G. S., and Reinhardt, P. W. Nondissociative electron capture in complex molecules and negative-ion lifetimes. *J. Chem. Phys.* 45: 4634 (1966).
  65. Wentworth, W. E., Becker, R. S., and Tung, R. Thermal electron attachment to some aliphatic and aromatic chloro, bromo, and iodo derivatives. *J. Phys. Chem.* 71: 1652 (1967).
  66. Chaney, E. L., and Christophorou, L. G. Electron attachment to  $N_2O$ . *J. Chem. Phys.* 51: 883 (1969).
  67. Wentworth, W. E., George, R., and Keith, H. Dissociative thermal electron attachment to some aliphatic chloro, bromo, iodo compounds. *J. Chem. Phys.* 51: 1791 (1969).
  68. Fehsenfeld, F. C. Electron attachment to  $SF_6$ . *J. Chem. Phys.* 53: 2000 (1970).
  69. Warman, J. M., and Sauer, M. C., Jr. The temperature dependence of electron attachment to  $CCl_4$ ,  $CH_3Cl$  and  $C_6H_5CH_2Cl$ . *Int. J. Rad. Phys. Chem.* 3: 273 (1971).
  70. O'Malley, T. F. Calculation of dissociative attachment in hot  $O_2$ . *Phys. Rev.* 155: 59 (1967).
  71. Chen, J. C. Y., and Peacher, J. L. Survival probability in dissociative attachment. *Phys. Rev.* 163: 103 (1967).
  72. Allan, M., and Wong, S. F. Dissociative attachment from vibrationally and rotationally excited  $H_2$  by electron impact. Abstracts of the Thirty-first Annual Gaseous Electronics Conference, Buffalo, New York, October 1978, paper MA-2, p. 125.
  73. Wadehra, J. M., and Bardsley, J. N. The dependence of the dissociative attachment on the vibrational and rotational state in  $e-H_2$  collisions. Abstracts of the Thirty-first Annual Gaseous Electronics Conference, Buffalo, New York, October 1978, paper MA-3, p. 126.
  74. Ferguson, E. E., Fehsenfeld, F. C., and Schmeltekopf, A. L. Geometrical considerations for negative ion processes. *J. Chem. Phys.* 47: 3085 (1967).
  75. Christodoulides, A. A., Christophorou, L. G., Pai, R. Y., and Tung, C. M. Electron attachment to perfluorocarbon compounds. I.  $c-C_4F_6$ ,  $2-C_4F_6$ ,  $1,3-C_4F_6$ ,  $c-C_4F_8$  and  $2-C_4F_8$ . *J. Chem. Phys.* 70: 1156 (1979).
  76. Pai, R. Y., Christophorou, L. G., and Christodoulides, A. A. Electron attachment to perfluorocarbon compounds. II.  $c-C_6F_8$ ,  $c-C_6F_{10}$ ,  $c-C_6F_{12}$ ,  $C_7F_8$  and  $C_8F_{16}$ : relevance to gaseous dielectrics. *J. Chem. Phys.* 70: 1169 (1979).
  77. Christophorou, L. G. Electron attachment to molecules in dense gases ("quasi-liquids"). *Chem. Rev.* 76: 409 (1976).
  78. Christophorou, L. G., McCorkle, D. L., and Anderson, V. E. Swarm-determined electron attachment cross sections as a function of electron energy. *J. Phys. B* 4: 1163 (1971).
  79. Christodoulides, A. A., and Christophorou, L. G. Electron attachment to perfluoromethylcyclohexane ( $c-C_7F_{14}$ ) and perfluoro-1-heptene ( $1-C_7F_{14}$ ). *Chem. Phys. Letters* 61: 553 (1979).
  80. Reese, R. M., Dibeler, V. H., and Mohler, F. L. Survey of negative ions in mass spectra of polyatomic molecules. *J. Res. Nat. Bur. Stand.* 57: 367 (1956).
  81. Fessenden, R. W., and Bansal, K. M. Direct observation of electron disappearance in pulse irradiated fluorocarbon gases. *J. Chem. Phys.* 53: 3468 (1970).
  82. Bansal, K. M., and Fessenden, R. W. Electron disappearance in pulse irradiated fluorocarbon gases. *J. Chem. Phys.* 59: 1760 (1973).
  83. Thynne, J. C. J. Negative ion studies using a time-of-flight mass spectrometer. *Dyn. Mass Spectrom.* 3: 67 (1972).
  84. Hammond, P. R. Electron-acceptor-electron-donor interactions. XVII. Concerning the electron affinities of sulfurhexafluoride and some other electron scavenging molecules. *J. Chem. Phys.* 55: 3468 (1971).
  85. Christodoulides, A. A., Schultes, E., Schumacher, R., and Schindler, R. N. An investigation of the molecules  $O_2$ ,  $CHCl_3$ ,  $c-C_4F_8$ ,  $C_7F_{14}$  and  $HBr$  by electron cyclotron resonance (ECR) technique at energies  $\leq 0.4$  eV. *Z. Naturforsch.* 29a: 389 (1974).
  86. Davis, F. J., Compton, R. N., and Nelson, D. R. Thermal energy electron attachment rate constants for some polyatomic molecules. *J. Chem. Phys.* 59: 2324 (1973).
  87. Harland, P. W., and Thynne, J. C. J. Ionization of perfluorocyclobutane by electron impact. *Int. J. Mass Spectrom. Ion Phys.* 10: 11 (1972/73).
  88. Henis, J. M. S., and Mabie, C. A. Determination of autoionization lifetimes by ion cyclotron resonances linewidths. *J. Chem. Phys.* 53: 2999 (1970).
  89. Christophorou, L. G., McCorkle, D. L., and Pittman, D. Electron attachment to  $CCl_2F_2$  and  $c-C_4F_8$  below  $\sim 2$  eV. *J. Chem. Phys.* 60: 1183 (1974).
  90. Mothes, K. G., Schultes, E., and Schindler, R. N. Application of electron cyclotron resonance technique in studies of electron capture processes in the thermal energy range. *J. Phys. Chem.* 76: 3758 (1972).
  91. Chen, C., George, R. D., and Wentworth, W. E. Experi-

- mental determination of rate constants for thermal electron attachment to gaseous  $\text{SF}_6$  and  $\text{C}_7\text{F}_{14}$ . *J. Chem. Phys.* 49: 1973 (1968).
92. Mahan, B. H., and Young, C. E. Gaseous thermal electron reactions: attachment to  $\text{SF}_6$  and  $\text{C}_7\text{F}_{14}$ . *J. Chem. Phys.* 44: 2192 (1966).
  93. Bansal, K. M., and Fessenden, R. W. Electron disappearance in pulse irradiated  $\text{CH}_3\text{Cl}$ ,  $\text{C}_2\text{H}_5\text{Cl}$ ,  $\text{CH}_3\text{Br}$  and  $\text{C}_2\text{H}_5\text{Br}$ . *Chem. Phys. Letters* 15: 21 (1972).
  94. Christodoulides, A. A., Schumacher, R., and Schindler, R. N. Studies by the electron cyclotron resonance technique. X. Interactions of thermal-energy electrons with molecules of chlorine, hydrogen chloride, and methyl chloride. *J. Phys. Chem.* 79: 1904 (1975).
  95. Schultes, E., Christodoulides, A. A., and Schindler, R. N. Studies by the electron cyclotron resonance (ECR) technique. VIII. Interactions of low-energy electrons with the chlorine-containing molecules  $\text{CCl}_4$ ,  $\text{CHCl}_3$ ,  $\text{CH}_2\text{Cl}_2$ ,  $\text{C}_n\text{H}_{2n+1}\text{Cl}$  ( $n = 1$  to 4),  $\text{C}_2\text{H}_3\text{Cl}$ ,  $\text{COCl}_2$ ,  $\text{NOCl}$ ,  $\text{CNCl}$  and  $\text{Cl}_2$ . *Chem. Phys.* 8: 354 (1975).
  96. Christodoulides, A. A., Schumacher, R., and Schindler, R. N. Studies by the electron cyclotron resonance (ECR) technique. IX. Interactions of low-energy electrons with the molecules  $\text{CH}_2\text{Cl}_2$  and  $\text{CHCl}_3$  in the gas phase. *Z. Naturforsch.* 30a: 811 (1975).
  97. Blaunstein, R. P., and Christophorou, L. G. Electron attachment to halogenated aliphatic hydrocarbons. *J. Chem. Phys.* 49: 1526 (1968).
  98. Christodoulides, A. A., and Christophorou, L. G. Electron attachment to brominated aliphatic hydrocarbons of the form  $n\text{-C}_n\text{H}_{2n+1}\text{Br}$  ( $n = 1$ -6, 8 and 10). I. An electron swarm study. *J. Chem. Phys.* 54: 4691 (1971).
  99. Bouby, L., Fiquet-Fayard, F., and Abgrall, H. Attache-ment d'electrons thermiques sur quelques vapeurs organiques. *Compt. Rend. Acad. Sci. (Paris)* 261: 4059 (1965).
  100. Schumacher, R., Sprünken, H.-R., Christodoulides, A. A., and Schindler, R. N. Studies by the electron cyclotron resonance technique. 13. Electron scavenging properties of the molecules  $\text{CCl}_3\text{F}$ ,  $\text{CCl}_2\text{F}_2$ ,  $\text{CClF}_3$  and  $\text{CF}_4$ . *J. Phys. Chem.* 82: 2248 (1978).
  101. Mothes, K. G., and Schindler, R. N. Die Bestimmung absoluter Geschwindigkeitskonstanten für den Einfang thermischer Elektronen durch  $\text{CCl}_4$ ,  $\text{SF}_6$ ,  $\text{C}_4\text{F}_8$ ,  $\text{C}_7\text{F}_{14}$ ,  $\text{N}_2\text{F}_4$  und  $\text{NF}_3$ . *Ber. Bunsenges Phys. Chem.* 75: 938 (1971).
  102. Johnson, J. P., McCorkle, D. L., Christophorou, L. G., and Carter, J. G. Long-lived parent negative ions formed via nuclear-excited Feshbach resonances. Part 4. — Systematic study of  $\text{NO}_2$ -containing benzene derivatives. *J. Chem. Soc. Faraday Trans. II*, 71: 1742 (1975).
  103. Hadjiantoniou, A., Christophorou, L. G., and Carter, J. G. Long-lived parent negative ions formed via nuclear-excited Feshbach resonances. Part 1.—Benzene derivatives. *J. Chem. Soc. Faraday Trans. II*, 69: 1691 (1973).
  104. Naff, W. T., Compton, R. N., and Cooper, C. D. Attachment of electrons to substituted benzenes. *J. Chem. Phys.* 54: 212 (1971).
  105. Christophorou, L. G., Carter, J. G., Chaney, E. L., and Collins, P. M. Long-lived parent negative ions formed by capture of low-energy electrons (0 to 3 eV) in the field of the ground and excited electronic states of organic molecules. *Proc. IVth Int. Congr. Rad. Res. (July 1970)*, Vol. 1, Physics and Chemistry, Duplan and Chapiro, Eds., Gordon and Breach, London, 1973, pp. 145-159.
  106. Goans, R. E., and Christophorou, L. G. Attachment of slow (<1 eV) electrons to  $\text{O}_2$  in very high pressures of nitrogen, ethylene and ethane. *J. Chem. Phys.* 60: 1036 (1974).
  107. Christophorou, L. G., and Goans, R. E. Low-energy (<1 eV) electron attachment to molecules in very-high pressure gases:  $\text{C}_6\text{H}_6$ . *J. Chem. Phys.* 60: 4244 (1974).
  108. Goans, R. E., and Christophorou, L. G. Low-energy ( $\leq 3$  eV) electron attachment to molecules in very-high pressure gases:  $\text{C}_2\text{H}_5\text{Br}$ . *J. Chem. Phys.* 63: 2821 (1975).
  109. Rademacher, J., Christophorou, L. G., and Blaunstein, R. P. Electron attachment to sulphur dioxide in high pressure gases. *J. Chem. Soc. Faraday Trans. II*, 71: 1212 (1975).
  110. Celotta, R. J., Bennett, R. A., and Hall, J. L. Laser photodetachment determination of the electron affinities of OH,  $\text{NH}_2$ , NH,  $\text{SO}_2$ , and  $\text{S}_2$ . *J. Chem. Phys.* 60: 1740 (1974).
  111. Christophorou, L. G. Interactions of  $\text{O}_2$  with slow electrons. *Rad. Phys. Chem.* 12: 19 (1978).
  112. Christophorou, L. G., and Blaunstein, R. P. Electron attachment in gases and liquids. *Chem. Phys. Letters* 12: 173 (1971).
  113. Christophorou, L. G. Mobilities of slow electrons in low- and high-pressure gases and liquids. *Int. J. Rad. Phys. Chem.* 7: 205 (1975).
  114. Christophorou, L. G., and McCorkle, D. L. Experimental evidence for the existence of a Ramsauer-Townsend minimum in liquid  $\text{CH}_4$  and liquid Ar (Kr and Xe). *Chem. Phys. Letters* 42: 533 (1976).
  115. Burrow, P. D., Dissociative attachment from the  $\text{O}_2$  ( $a^1\Delta_g$ ) state. *J. Chem. Phys.* 59: 4922 (1973).
  116. Hotop, H., and Lineberger, W. C. Binding energies in atomic negative ions. *J. Phys. Chem. Ref. Data* 4: 539 (1975).
  117. Blaunstein, R. P. and Christophorou, L. G. On molecular parameters of physical, chemical and biological interest. *Rad. Res. Revs.* 3: 69 (1971).
  118. Franklin, J. L., and Harland, P. W. Gaseous negative ions. *Ann. Rev. Phys. Chem.* 25: 485 (1974).
  119. Rosenstock, H. M., Draxl, K., Steiner, B. W., and Herron, J. T. Energetics of gaseous ions. *J. Phys. Chem. Ref. Data* 6 (Suppl. 1): (1977).
  120. Zimmerman, A. H., Reed, K. J., and Brauman, J. E. Photodetachment of electrons from enolate anions. Gas phase electron affinities of enolate radicals. *J. Am. Chem. Soc.* 99: 7203 (1977).
  121. Engelking, P. C., Ellison, G. B., and Lineberger, W. C. Laser photodetachment electron spectrometry of methoxide, deuteromethoxide, and thiomethoxide: Electron affinities and vibrational structure of  $\text{CH}_3\text{O}$ ,  $\text{CD}_3\text{O}$  and  $\text{CH}_3\text{S}$ . *J. Chem. Phys.* 69: 1826 (1978).
  122. Richardson, J. H., Stephenson, L. M., and Brauman, J. I. Photodetachment of electrons from large molecular systems: benzyl anion. An upper limit to the electron affinity of  $\text{C}_6\text{H}_5\text{CH}_2$ . *J. Chem. Phys.* 63: 74 (1975).
  123. Chupka, W. A., Berkowitz, J., and Gutman, D. Electron affinities of halogen diatomic molecules as determined by endoergic charge transfer. *J. Chem. Phys.* 55: 2724 (1971).
  124. Berkowitz, J., Chupka, W. A., and Gutman, D. Electron affinities of  $\text{O}_2$ ,  $\text{O}_3$ , NO,  $\text{NO}_2$ ,  $\text{NO}_3$  by endothermic charge transfer. *J. Chem. Phys.* 55: 2733 (1971).
  125. Tang, S. Y., Mathur, B. P., Rothe, E. W., and Reck, G. P. Negative ion formation in halocarbons by charge exchange with cesium. *J. Chem. Phys.* 64: 1270 (1976).
  126. Compton, R. N., Reinhardt, P. W., and Cooper, C. D. Collisional ionization between alkali atoms and some methane

- derivatives: electron affinities for  $\text{CH}_3\text{NO}_2$ ,  $\text{CF}_3\text{I}$  and  $\text{CF}_3\text{Br}$ . *J. Chem. Phys.* 68: 4360 (1978).
127. McNamee, P. E., Lacmann, K., and Herschbach, D. R. *Faraday Discuss. Chem. Soc.* 55: 318 (1973).
128. Dispert, H., and Lacmann, K. Negative ion formation in collisions between potassium and fluoro- and chloromethanes: electron affinities and bond dissociation energies. *Int. J. Mass Spectrom. Ion Phys.* 28: 49 (1978).
129. Simons, J. Theoretical studies of negative molecular ions. *Ann. Rev. Phys. Chem.* 28: 15 (1977).